Understanding Mid- and High-Latitude Ocean and Climate Dynamics from Long-term Satellite Altimetry Measurements

Bo Qiu

Department of Oceanography
University of Hawaii

Satellite Altimetry vs. Mid- and High-Latitude Ocean Circulation

- Regional descriptions of meso-scale eddy variability and its seasonal-to-decadal modulations
- Eddy-mean flow interaction along major ocean currents (e.g. WBCs, ACC, STCCs, Agulhas Retroflection)
- Monitoring the surface transport of major ocean currents and the strength of gyres
- Eastern boundary current variability – local forcing vs. ENSO-related remote forcing
- Wind-driven high-frequency barotropic signals in subpolar ocean basins
- Time-dependent Sverdrup response to large-scale wind forcing in subpolar ocean basins
- Inter-gyre / inter-basin eddy flux transport
- Ocean's roles in mid- and high-latitude climate variability

Ocean's Roles in Mid- and High-Latitude Climate Variability

- Through manifestation of ENSO, ocean's role in the coupled climate system has been well demonstrated in the tropics.
- Ocean's impact upon the mid- and high-latitude climate system is less well established (especially from observations).
- Long-term satellite altimetry measurements can play an essential role in enhancing our understanding of the mid- and high-latitude coupled climate system.

Point 1

- **Long-term SSH measurements from satellite altimeters provide a global data base that can lead to new physical insights into our understanding of mid- and high-latitude climate phenomena.**

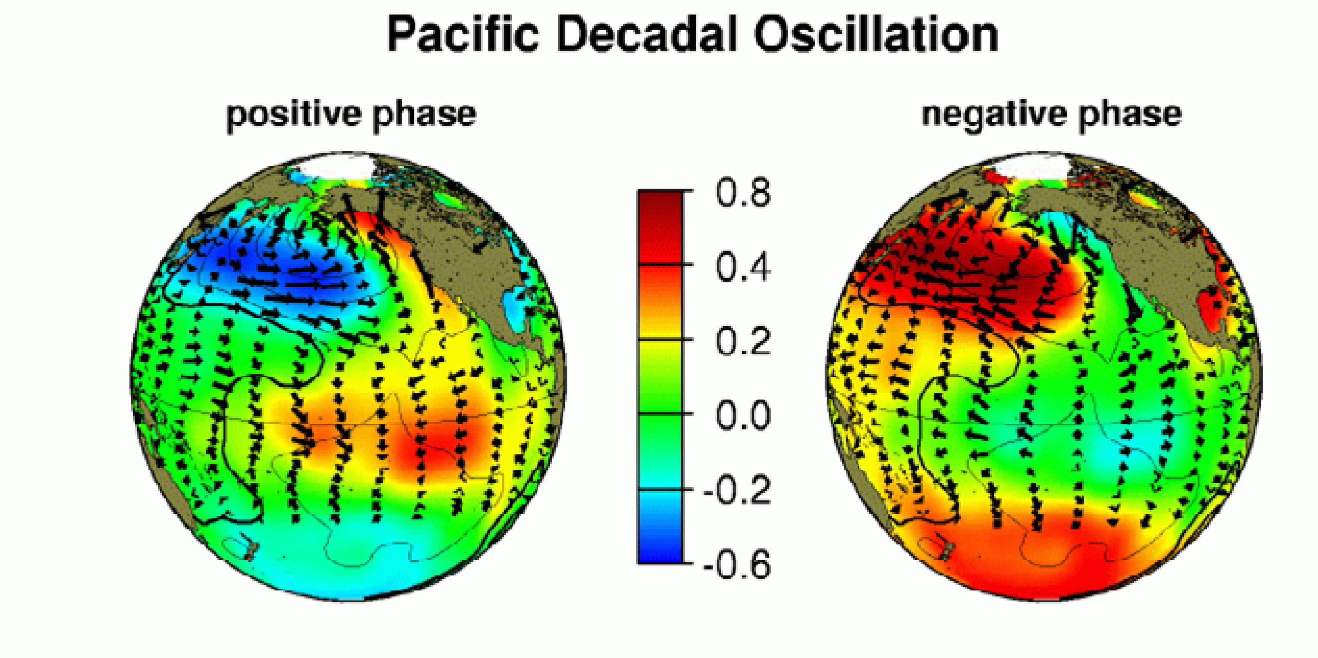

PDO Index (Mantua et al.)

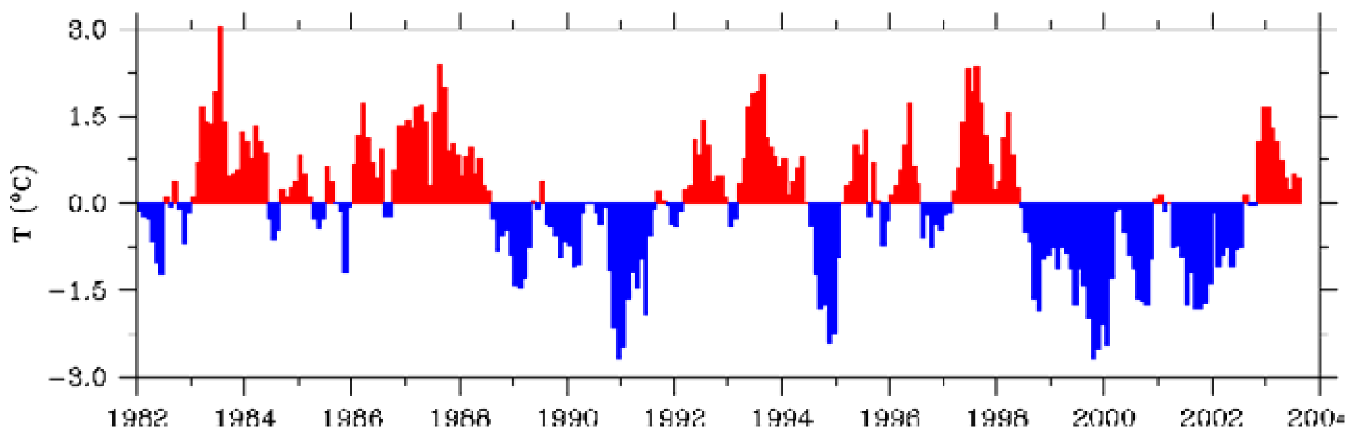

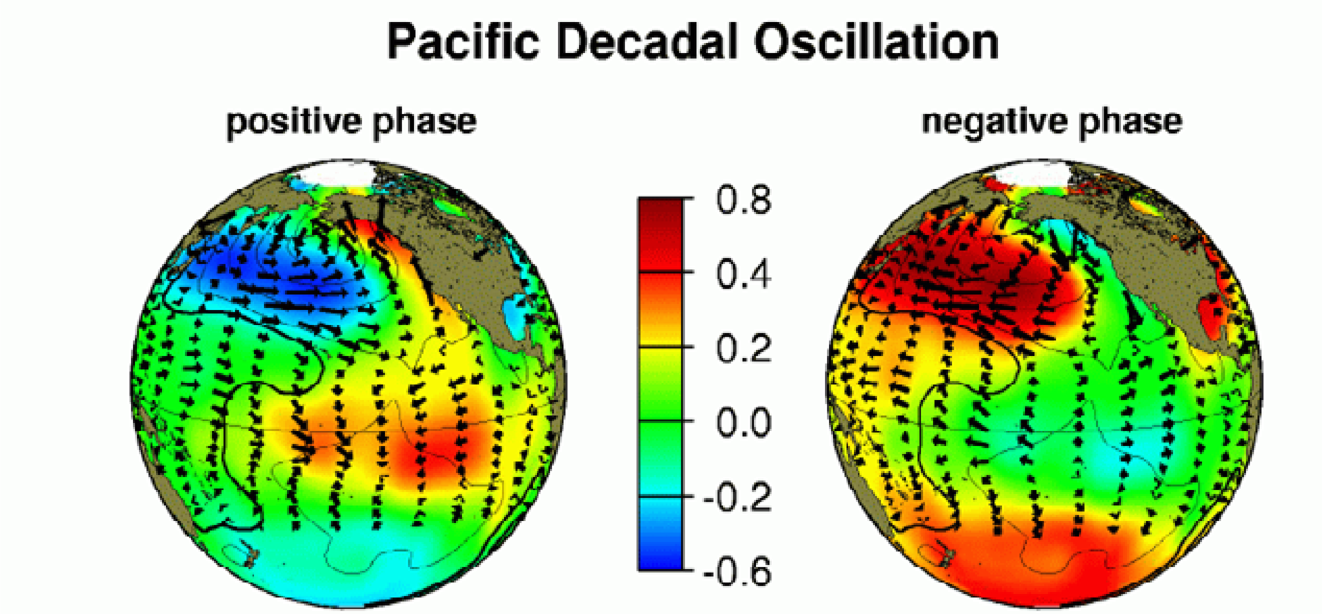

T/P, ERS-1/2, Jason-1

PDO Index

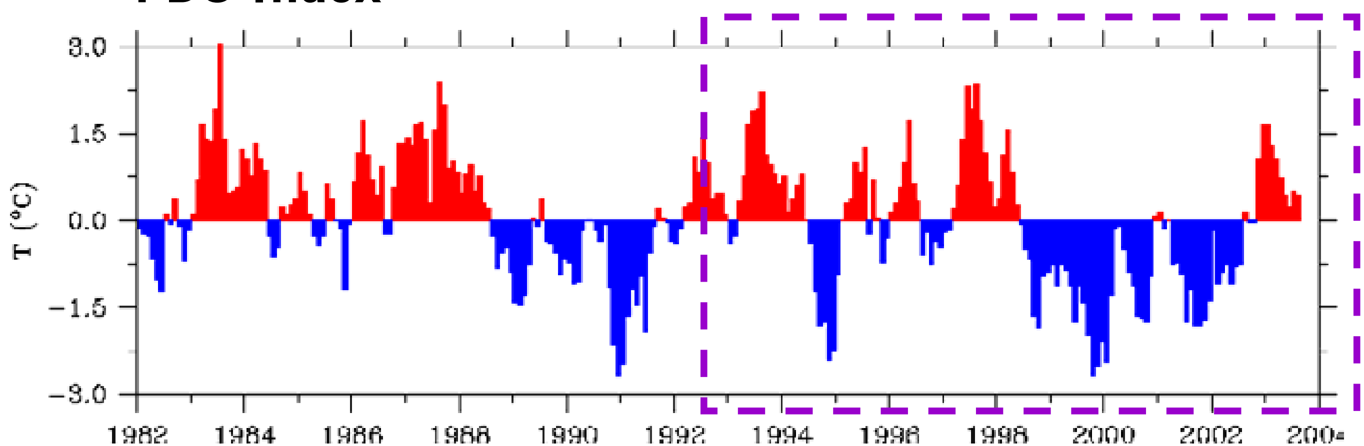

NCEP Wind Stress Curl: EOF Mode 1

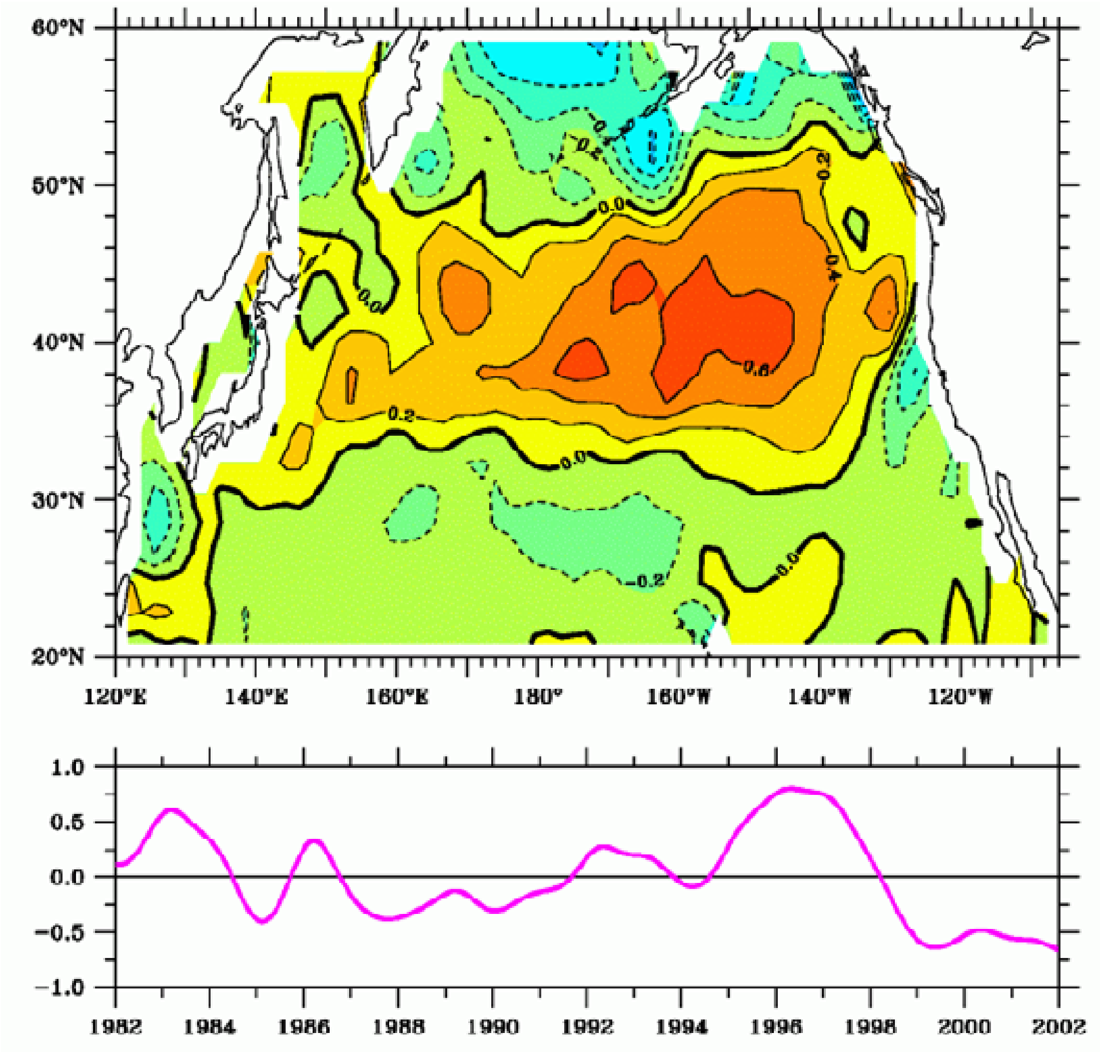

RMS Amplitude of Interannual SSH Signals (AVISO)

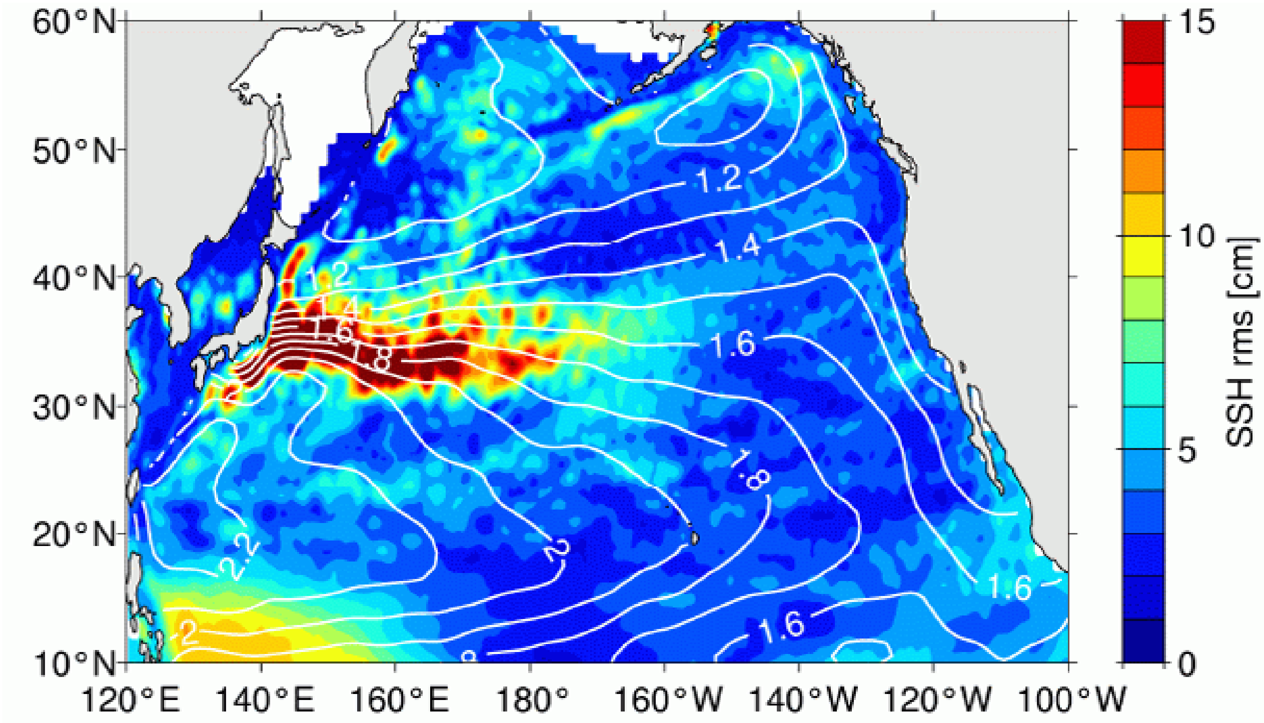

(white contours: mean SSH)

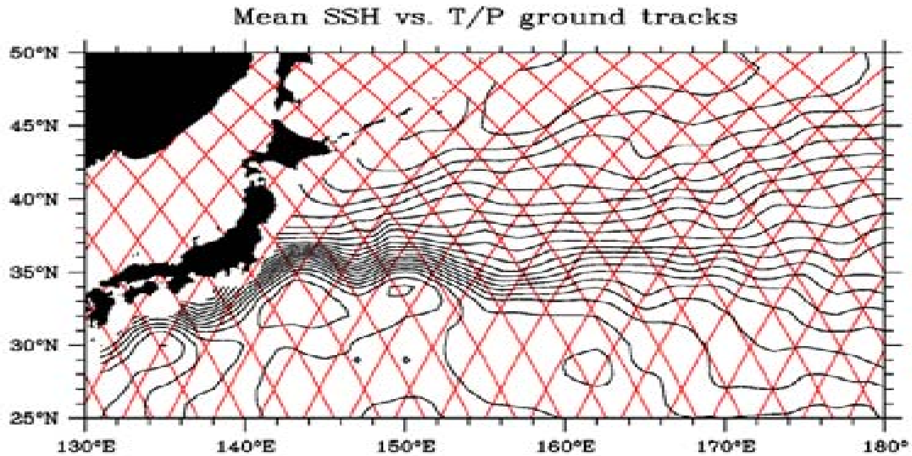
Mean SSH vs. T/P ground tracks
50°N
45°N
40°N
35°N
30°N
25°N
130°E
140°E
150°E
160°E
170°E
180°

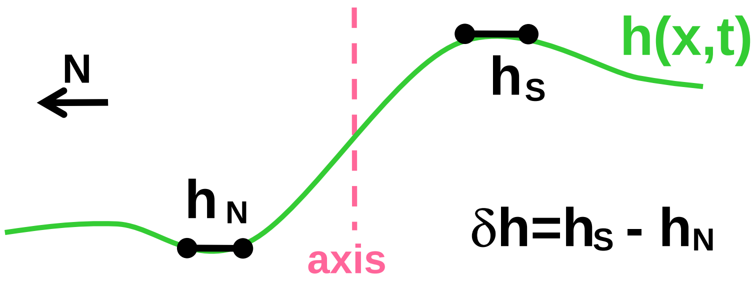
N
h(x,t)
h N
h S
axis
δh=hS - hN

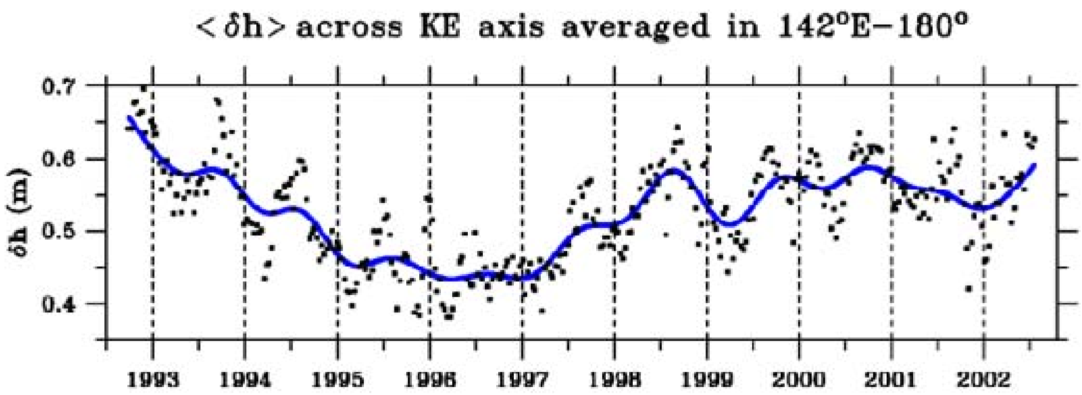
< δh > across KE axis averaged in 142°E–180°
δh (m)
0.7
0.6
0.5
0.4
1993
1994
1995
1996
1997
1998
1999
2000
2001
2002

T/P Yearly SSHA Fields

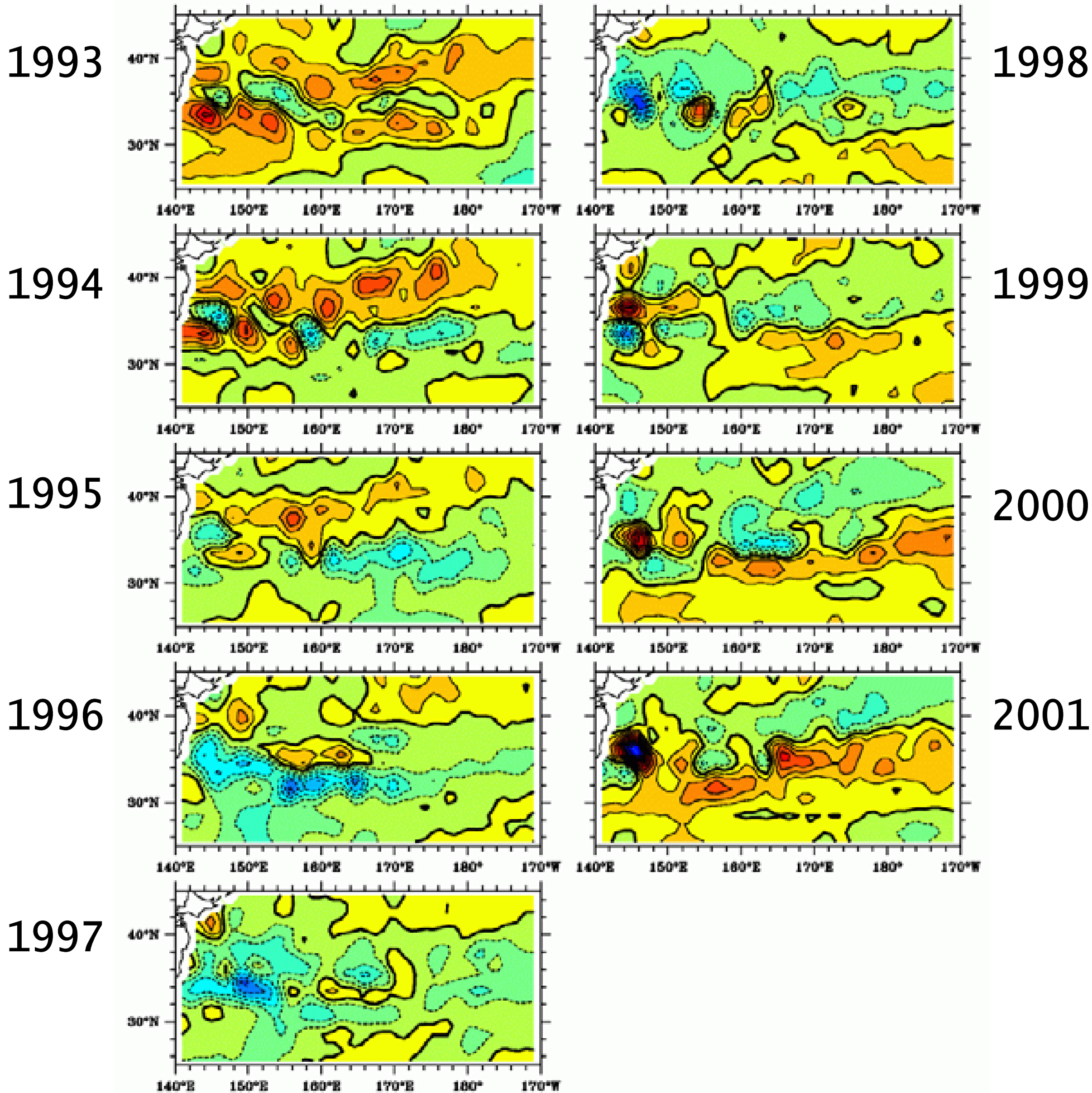

Dynamic Model

- Interested in the baroclinic upper ocean response due to basin-scale surface wind forcing.

- Under the longwave approximation (cf. local $L_R \simeq 35$ km), large-scale SSH, h, changes are governed by the linear vorticity equation:

$$\boxed{\frac{\partial h}{\partial t} - c_R \frac{\partial h}{\partial x} = -\frac{g' \nabla \times \boldsymbol{\tau}}{\rho_o g f},} \qquad (1)$$

  where c_R: speed of long baroclinic Rossby waves.

- Integrating Eq. (1) from the eastern boundary x_e along the wave characteristic:

$$\boxed{h(x,t) = h\left(x_e, t + \frac{x - x_e}{c_R}\right) + \frac{g'}{\rho_o g f c_R} \int_{x_e}^{x} \nabla \times \boldsymbol{\tau}\left(x', t + \frac{x - x'}{c_R}\right) dx'}$$

- To hindcast the $h(x,t)$ field:

  c_R: evaluated from the T/P data,

  $\nabla \times \boldsymbol{\tau}$: monthly data from NCEP reanalysis,

  $h(x_e, t) = 0$: no eastern boundary forcing (see Fu and Qiu, 2002)

T/P-derived C_R vs. Latitude

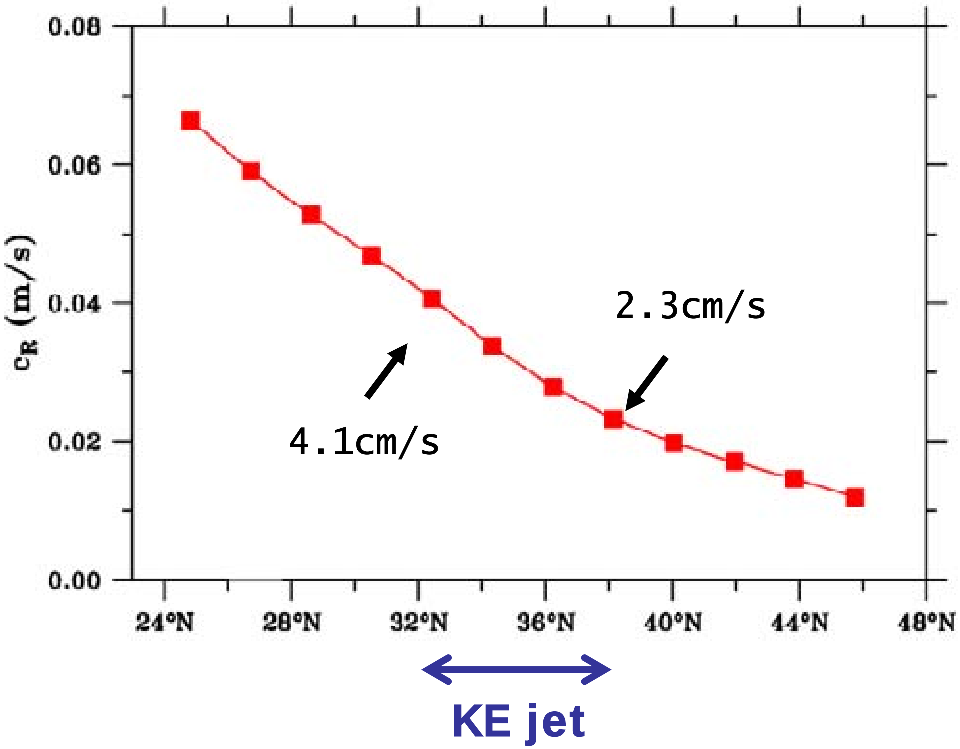

Note: $C_R=\beta g' H_e/f^2$; $f_N^2/f_S^2 = 1.33$

(cf. Chelton and Schlax 1996)

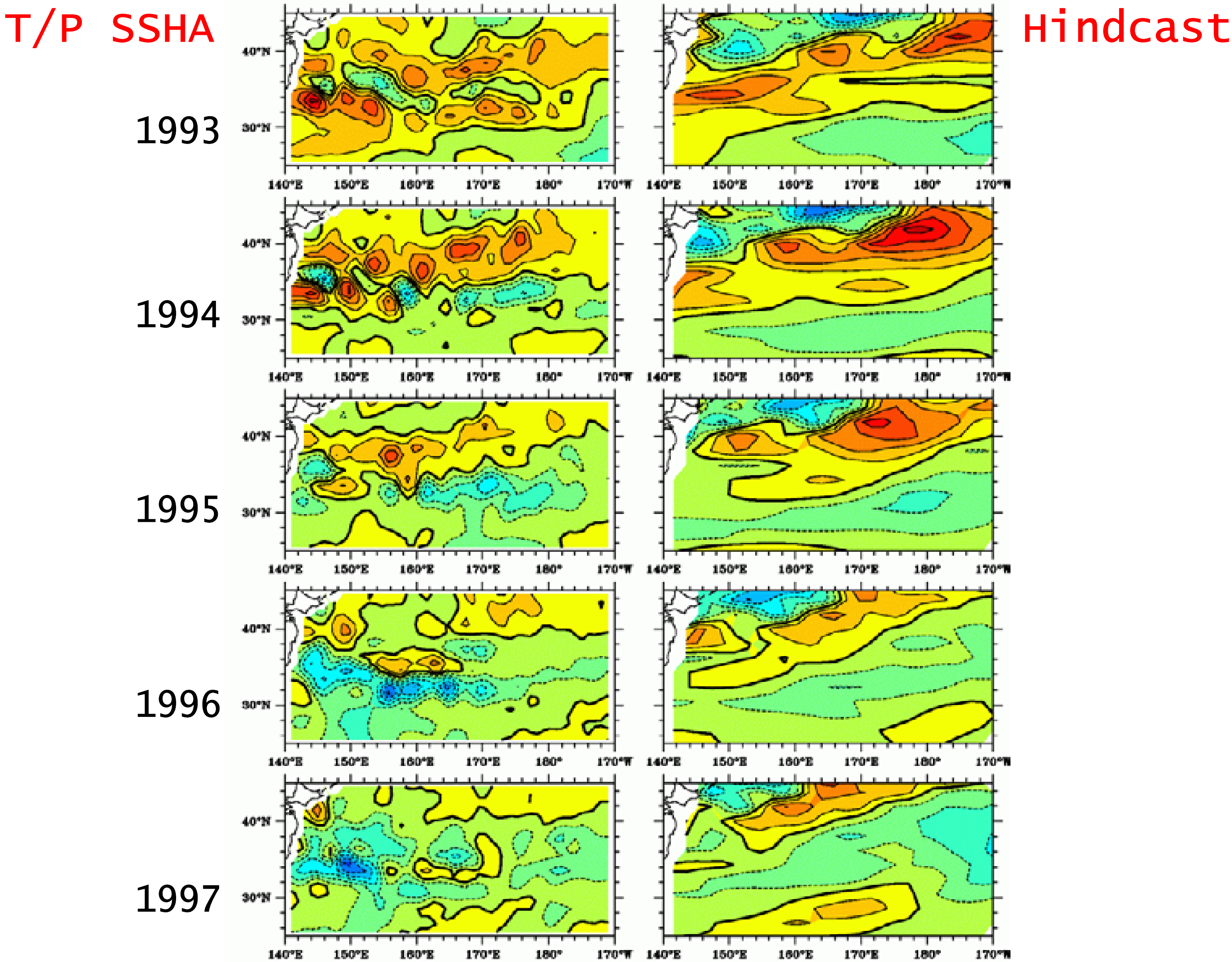
T/P SSHA
Hindcast
1993
1994
1995
1996
1997
40°N
30°N
140°E
150°E
160°E
170°E
180°
170°W

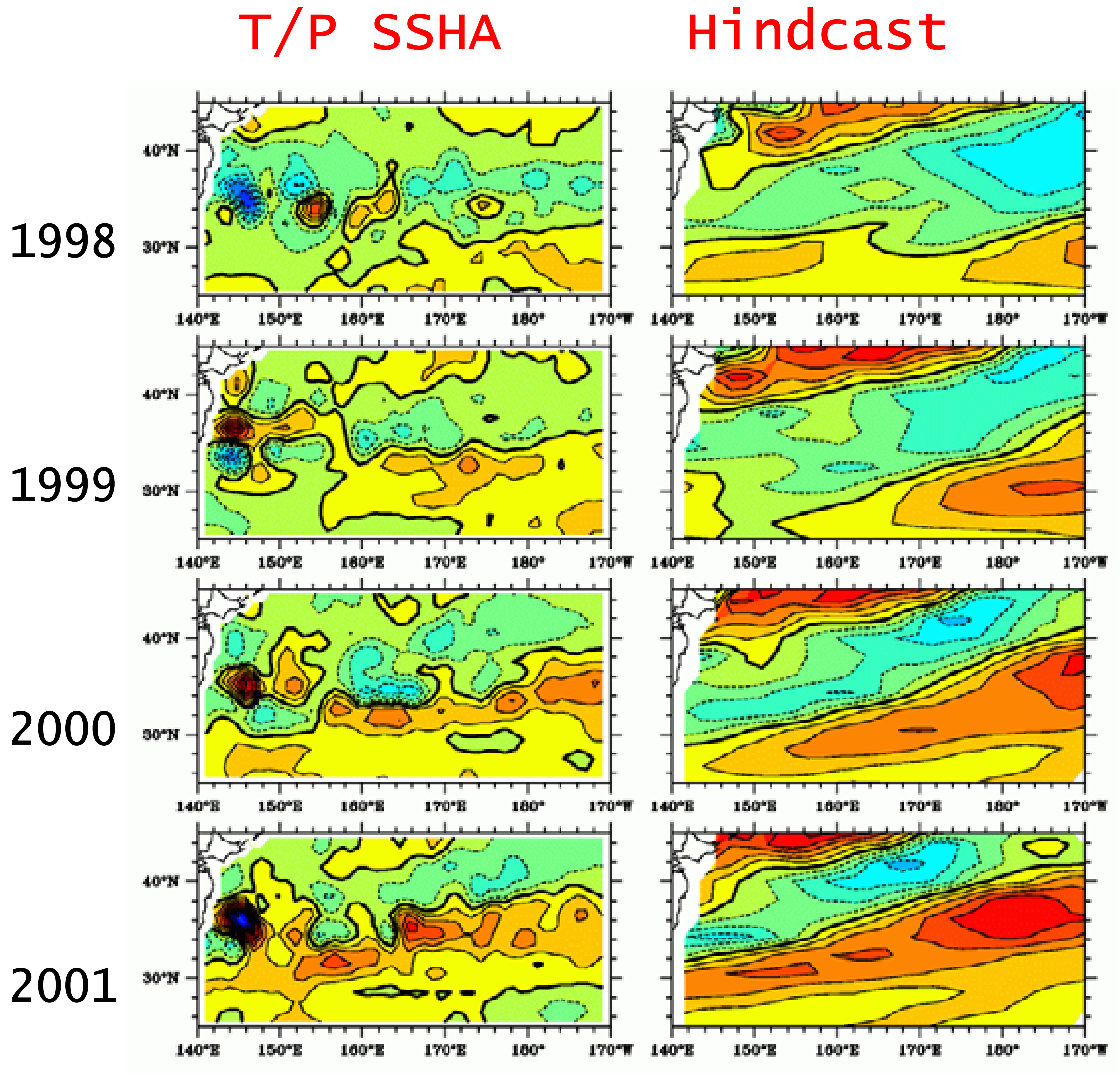
T/P SSHA
Hindcast
1998
1999
2000
2001
40°N
30°N
140°E
150°E
160°E
170°E
180°
170°W

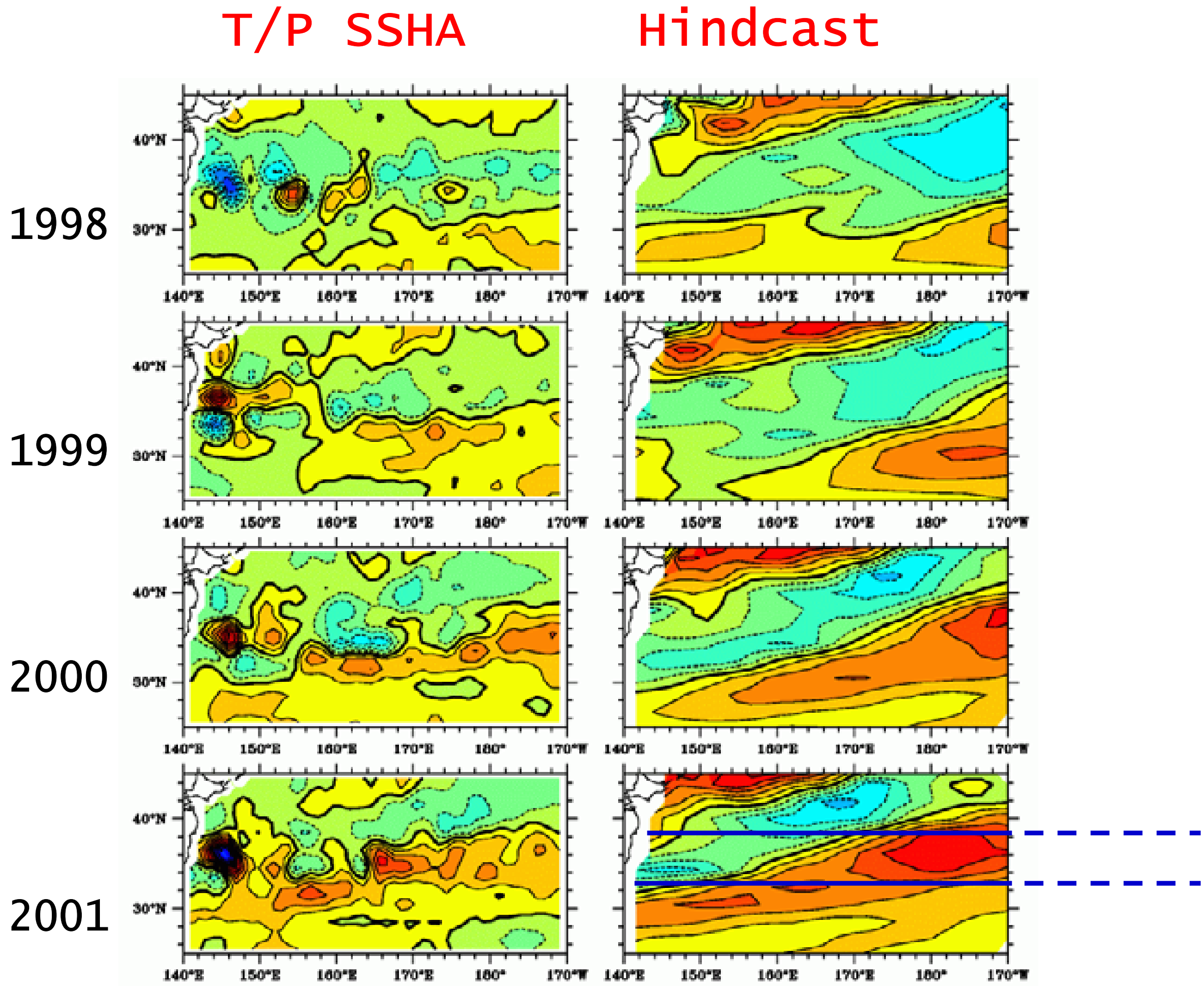
T/P SSHA
Hindcast
1998
1999
2000
2001
40°N
30°N
140°E
150°E
160°E
170°E
180°
170°W

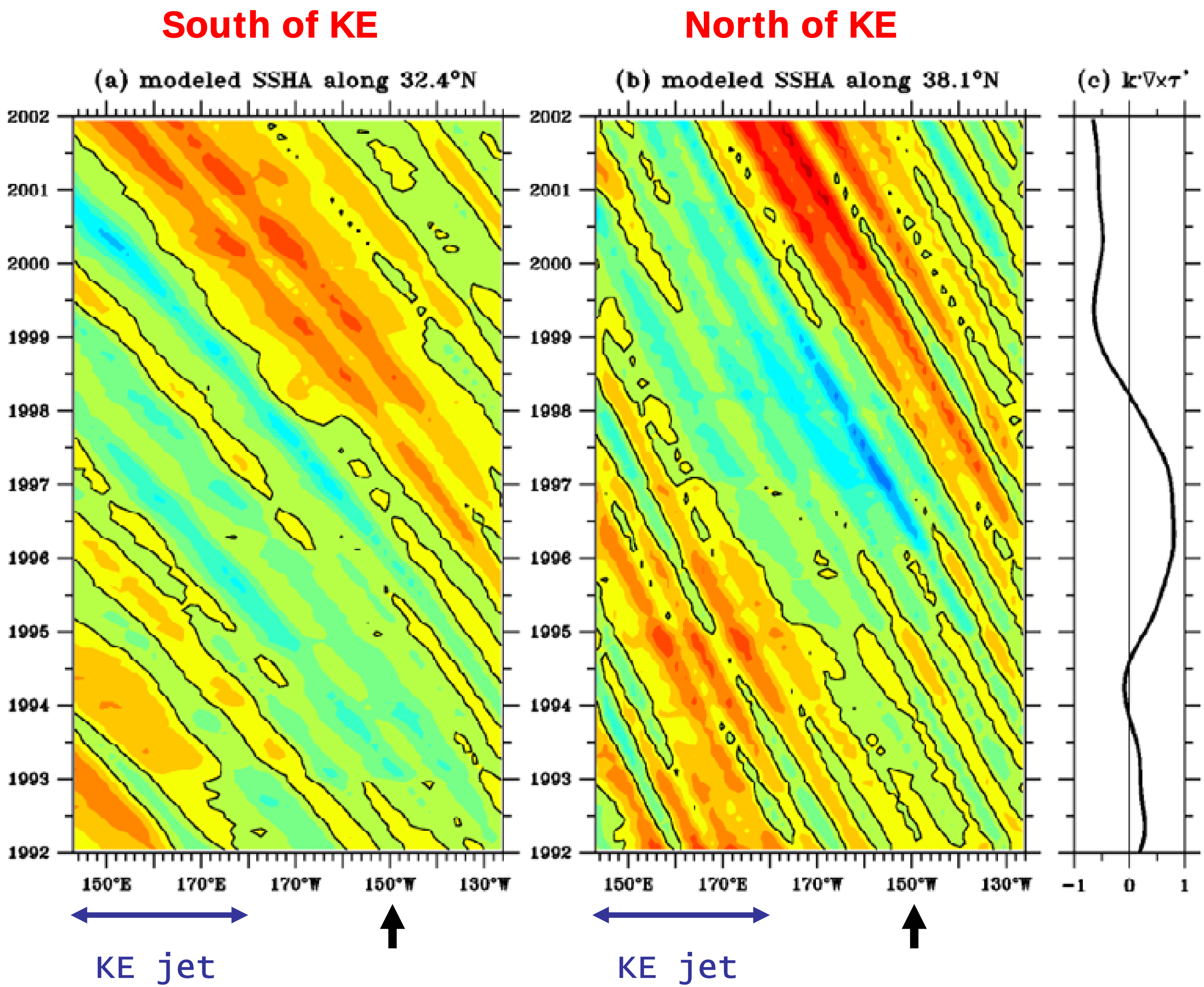

South of KE
North of KE
(a) modeled SSHA along 32.4°N
(b) modeled SSHA along 38.1°N
(c) k·∇×τ'
2002
2001
2000
1999
1998
1997
1996
1995
1994
1993
1992
150°E
170°E
170°W
150°W
130°W
−1
0
1
KE jet
KE jet

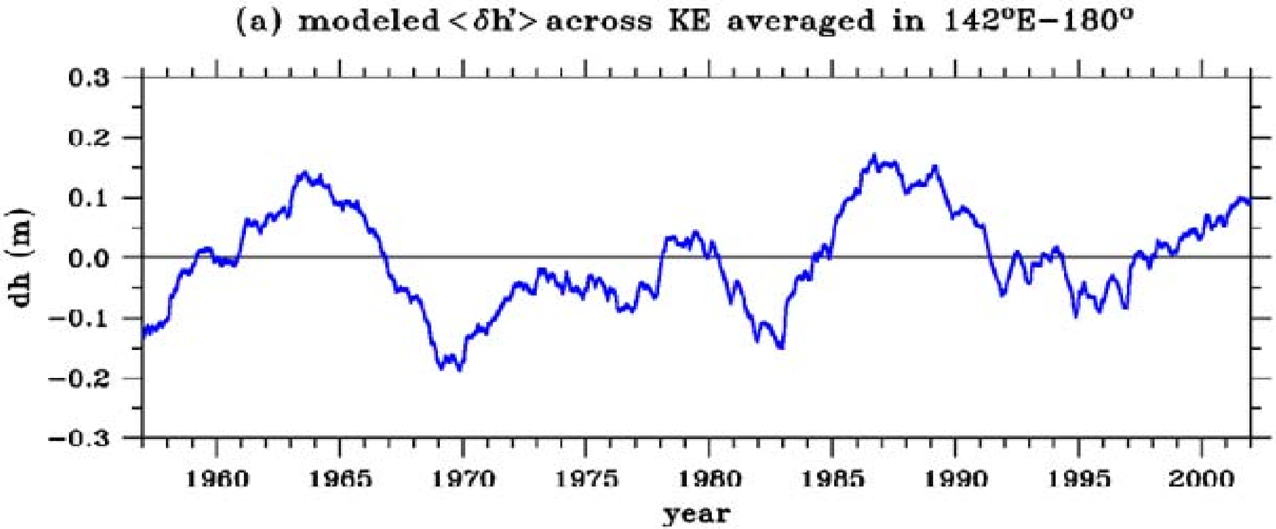

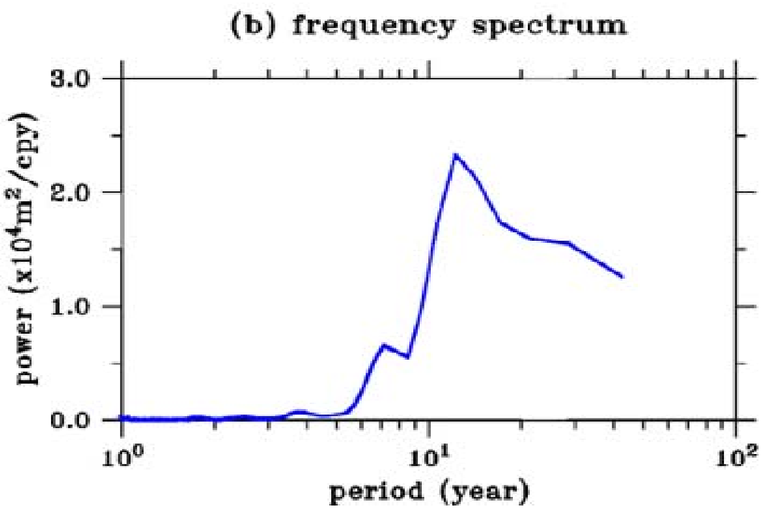

1yr. 10yr. 100yr.

Hindcast using

NCEP wind stress

data: 1948-2001

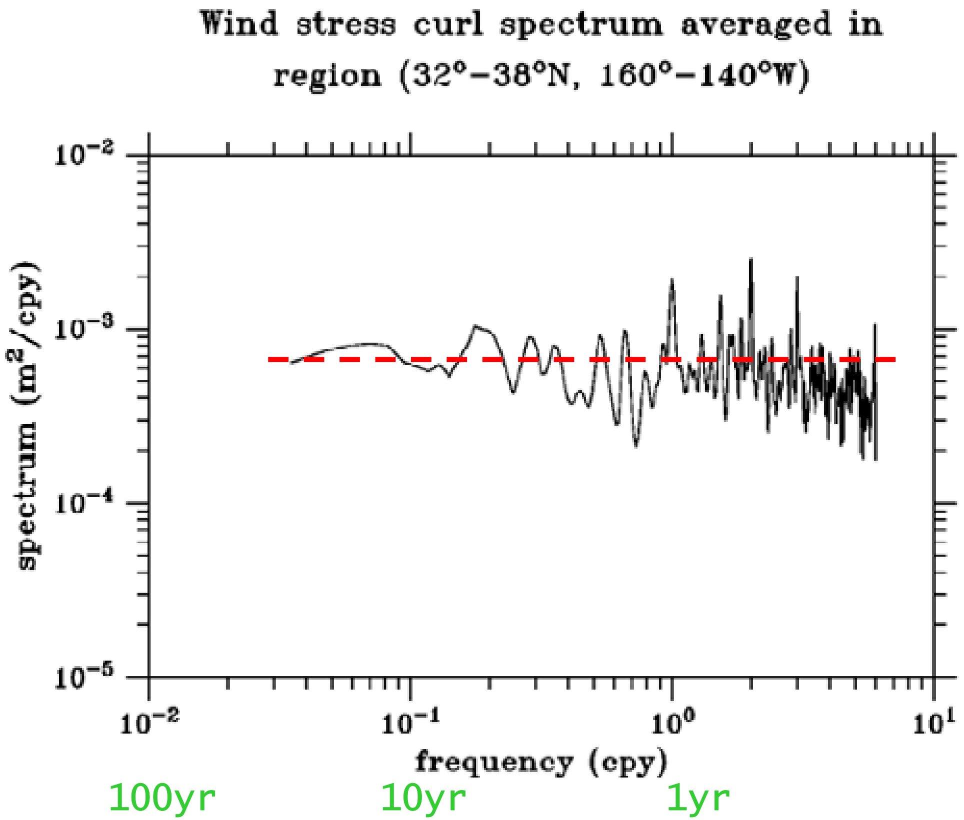

NCEP reanalysis: 1948-2001

Magnitude of the wind-forced $\langle \delta h' \rangle$ across the Kuroshio Ext. jet is sensitive to the period of the wind forcing.

- **Consider the following stochastic forcing problem:**

$$\frac{\partial h'}{\partial t} - c_R \frac{\partial h'}{\partial x} = F(x)W(t),$$

where the wind forcing has a "white" spectrum in time. For simplicity, let $F(x) = \delta(x - x_o)$ and $x_o = 0$.

“White” forcing in the east

- **West of $x_o = 0$:**

$$h'(x,t) = \frac{1}{c_R}\int_x^0 F(x')\,W\left(t + \frac{x - x'}{c_R}\right)dx' = \frac{1}{c_R}W\left(t + \frac{x}{c_R}\right).$$

- **Averaging h' over the jet length L along latitude A:**

$$\langle h'_A \rangle(t) = \frac{1}{L}\int_{-C-L/2}^{-C+L/2}\frac{1}{c_{RA}}W\left(t + \frac{x}{c_{RA}}\right)dx$$

and taking the Fourier transform:

$$\langle \widehat{h'_A} \rangle(\omega) = \frac{2}{\omega L}\widehat{W}(\omega)\sin\left(\frac{\omega L}{2c_{RA}}\right)\exp\left(\frac{i\omega C}{c_{RA}}\right).$$

- **Similarly, along latitude B:**

$$\langle \widehat{h'_B} \rangle(\omega) = \frac{2}{\omega L}\widehat{W}(\omega)\sin\left(\frac{\omega L}{2c_{RB}}\right)\exp\left(\frac{i\omega C}{c_{RB}}\right).$$

- Taking the SSH difference across the zonal jet, the power spectrum for $\langle \delta h' \rangle$ under $|\widehat{W}(\omega)|^2 = 1$ is:

$$\boxed{\begin{aligned} |\langle \widehat{\delta h'} \rangle(\omega)|^2 = \frac{T^2}{\pi^2 L^2}\Bigg[\sin^2\left(\frac{\pi L}{T c_{RA}}\right) + \sin^2\left(\frac{\pi L}{T c_{RB}}\right) \\ -2\sin\left(\frac{\pi L}{T c_{RA}}\right)\sin\left(\frac{\pi L}{T c_{RB}}\right)\cos\left(\frac{2\pi C}{T c_{RB}} - \frac{2\pi C}{T c_{RA}}\right)\Bigg]. \end{aligned}}$$

KE response power

- In the high-freq limit, the power spectrum has an upper bound:

$$|\langle \widehat{\delta h'} \rangle(\omega)|^2 \le \frac{4T^2}{\pi^2 L^2},$$

which increases with the forcing period T.

- In the low-freq limit, the power spectrum simplifies to:

$$|\langle \widehat{\delta h'} \rangle(\omega)|^2 \sim \left(1 + \frac{4\pi^2 C^2}{c_{RB} c_{RA} T^2}\right)\left(\frac{1}{c_{RB}} - \frac{1}{c_{RA}}\right)^2,$$

which decreases with increasing T.

- In between these two limits, an optimum T exists for which $|\langle \widehat{\delta h'} \rangle|^2$ is a maximum. Using values appropriate for the N Pacific, we have:

$$\boxed{T_{optimum} \sim 10 \text{ yrs.}}$$

Optimum forcing period

- This "preferred" forcing period is *not* very sensitive to the detailed values of the chosen C, L, A and B.

Power spectra under "white" freq forcing
$F(x)=\delta(x-x_o)$ vs. $F(x)=\exp[-(x-x_o)^2/a^2]$

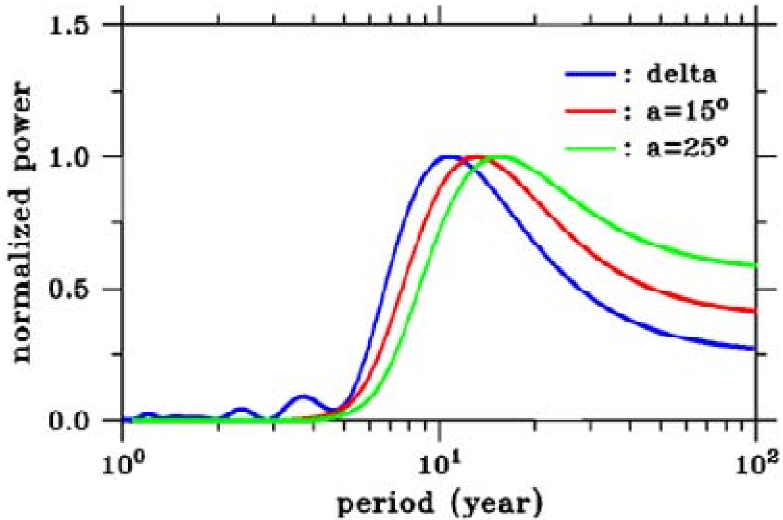

Theory

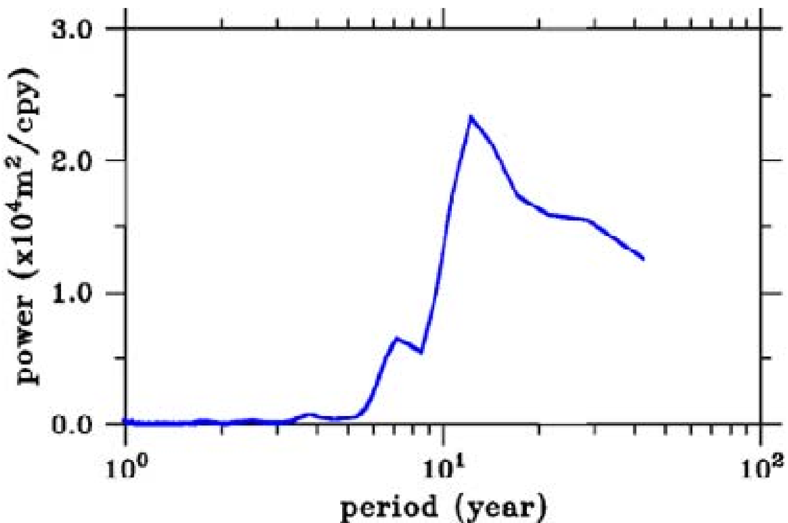

NCEP wind hindcast

Forced SSHA Patterns

(contour interval: pi)

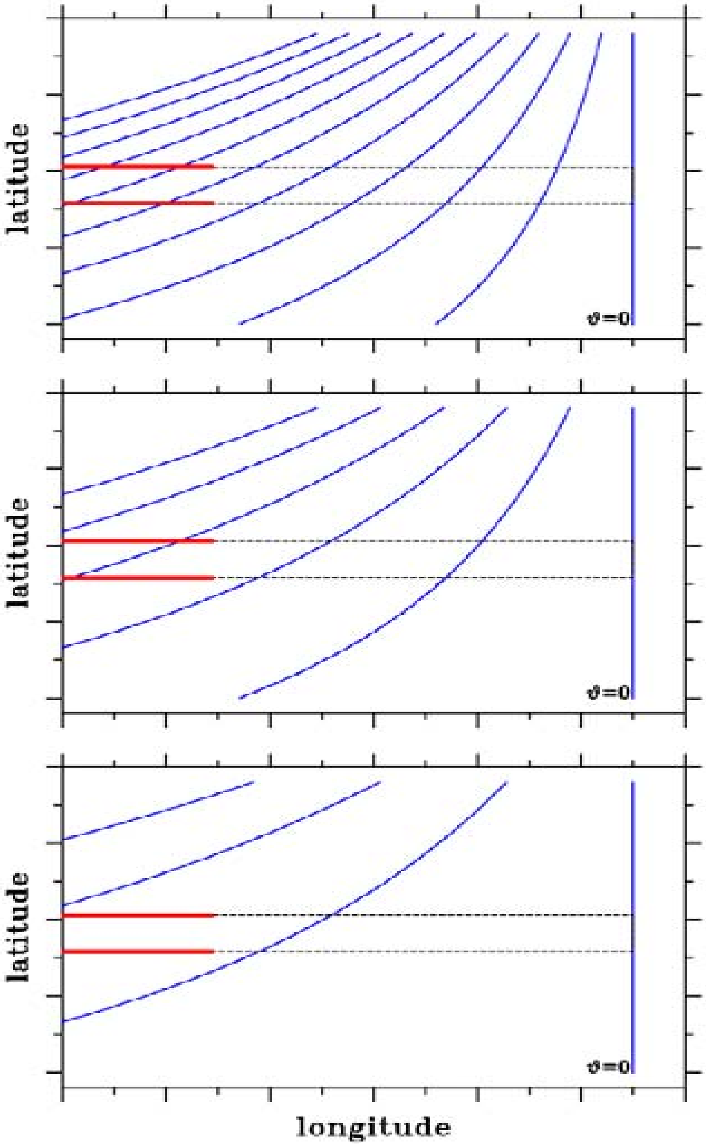

T: short

T: intermediate

T: long

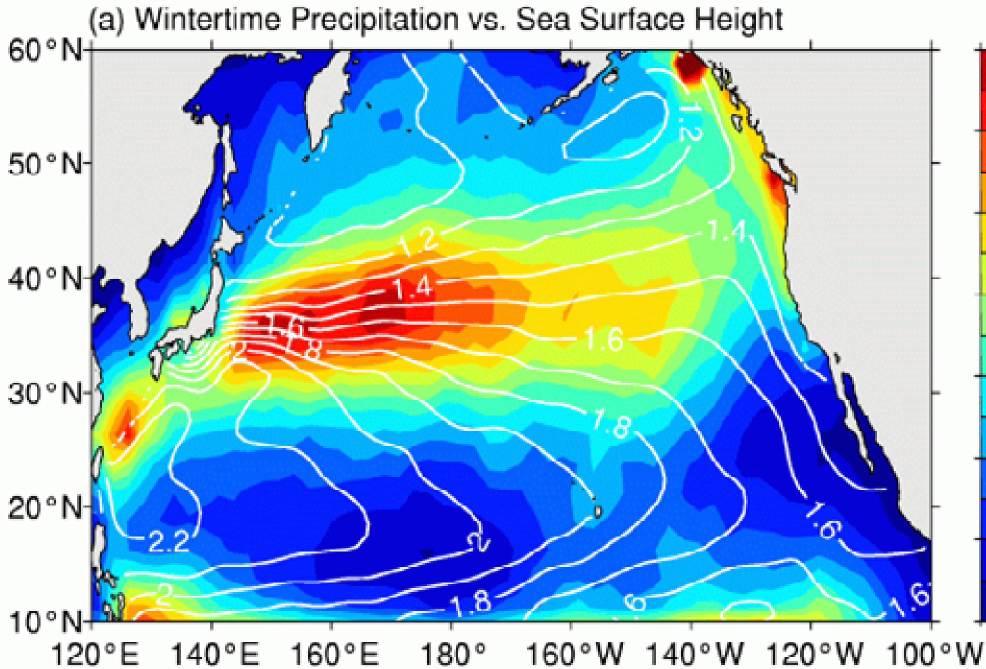
(a) Wintertime Precipitation vs. Sea Surface Height
60°N
50°N
40°N
30°N
20°N
10°N
120°E
140°E
160°E
180°
160°W
140°W
120°W
100°W
Precipitation [mm/yr]
0
1
2
3
4
5
6
7

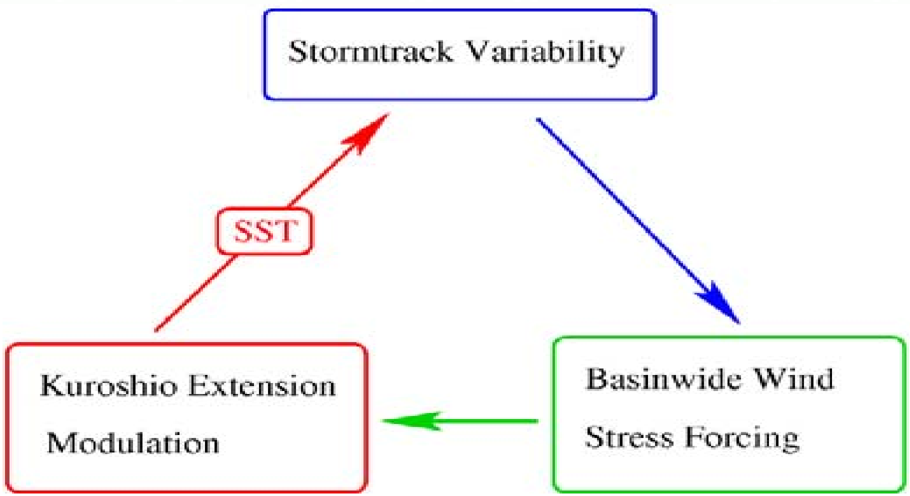
Stormtrack Variability
SST
Kuroshio Extension Modulation
Basinwide Wind Stress Forcing

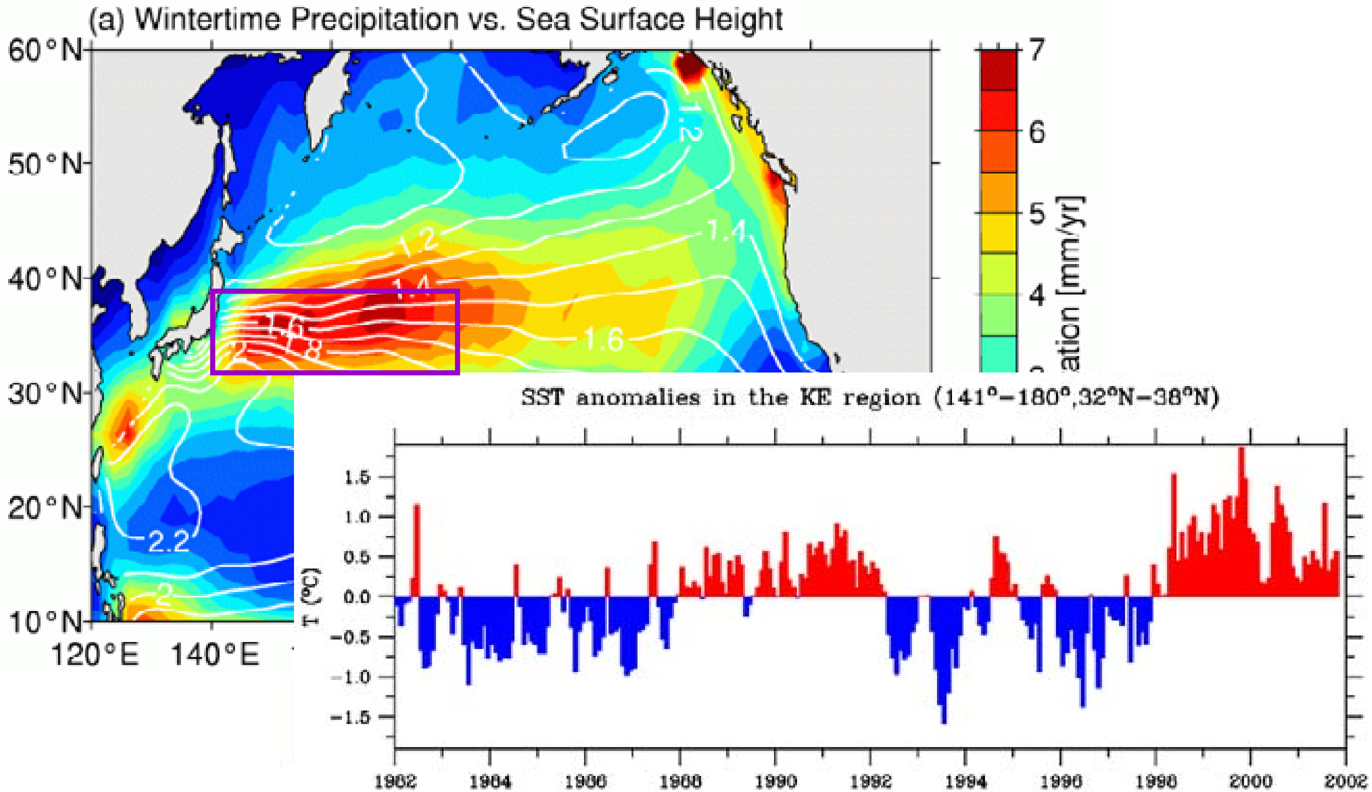

Vivier et al. (2002)

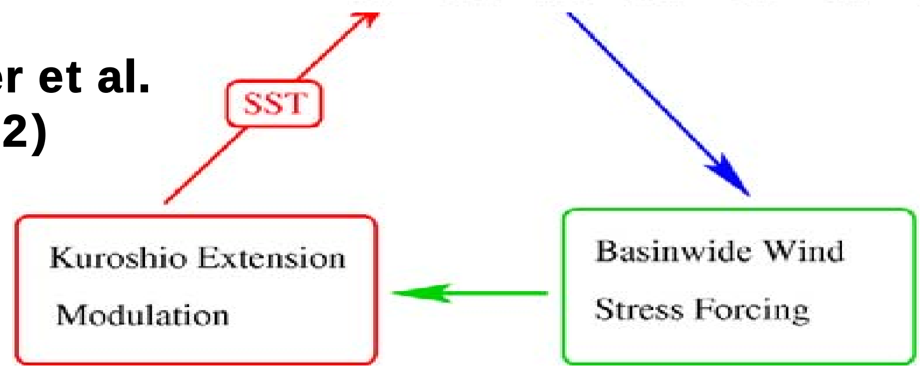

Summary of Point 1

- **Given the relative positions between the atmos. forcing and the KE jet, the lagged oceanic response across the KE jet preferentially enhances the *decadal* timescale variability.**
- **This insight regarding the KE jet modulation stems from the detailed SSH information provided by the long-term satellite altimeter data.**
- **Continued SSH measurements will provide more new insights into our understanding of the mid- and high-latitude climate phenomena.**

Point 2

- **Long-term SSH measurements from satellite altimeters can be used to test dynamic hypotheses underlying an observed physical phenomenon.**

ACWs: Is it a coupled phenomenon ?

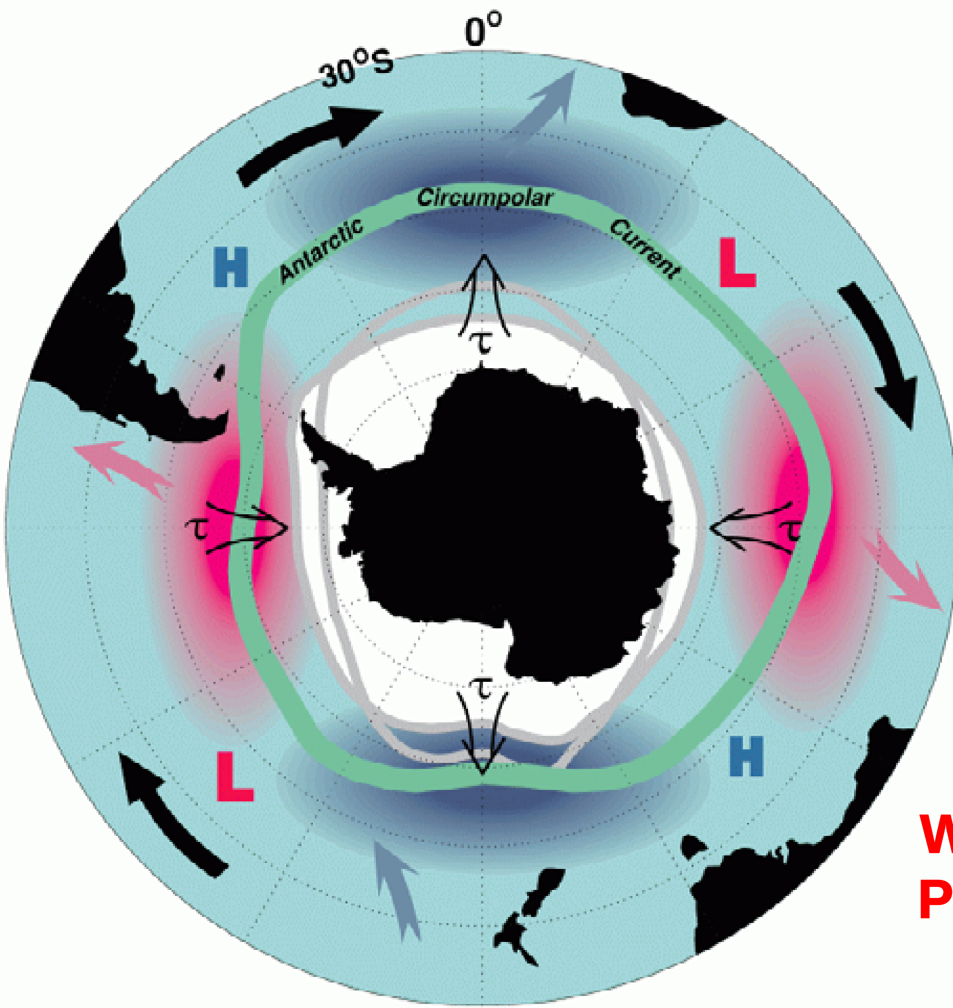

White and Peterson (1996)

White and Chen (2002)

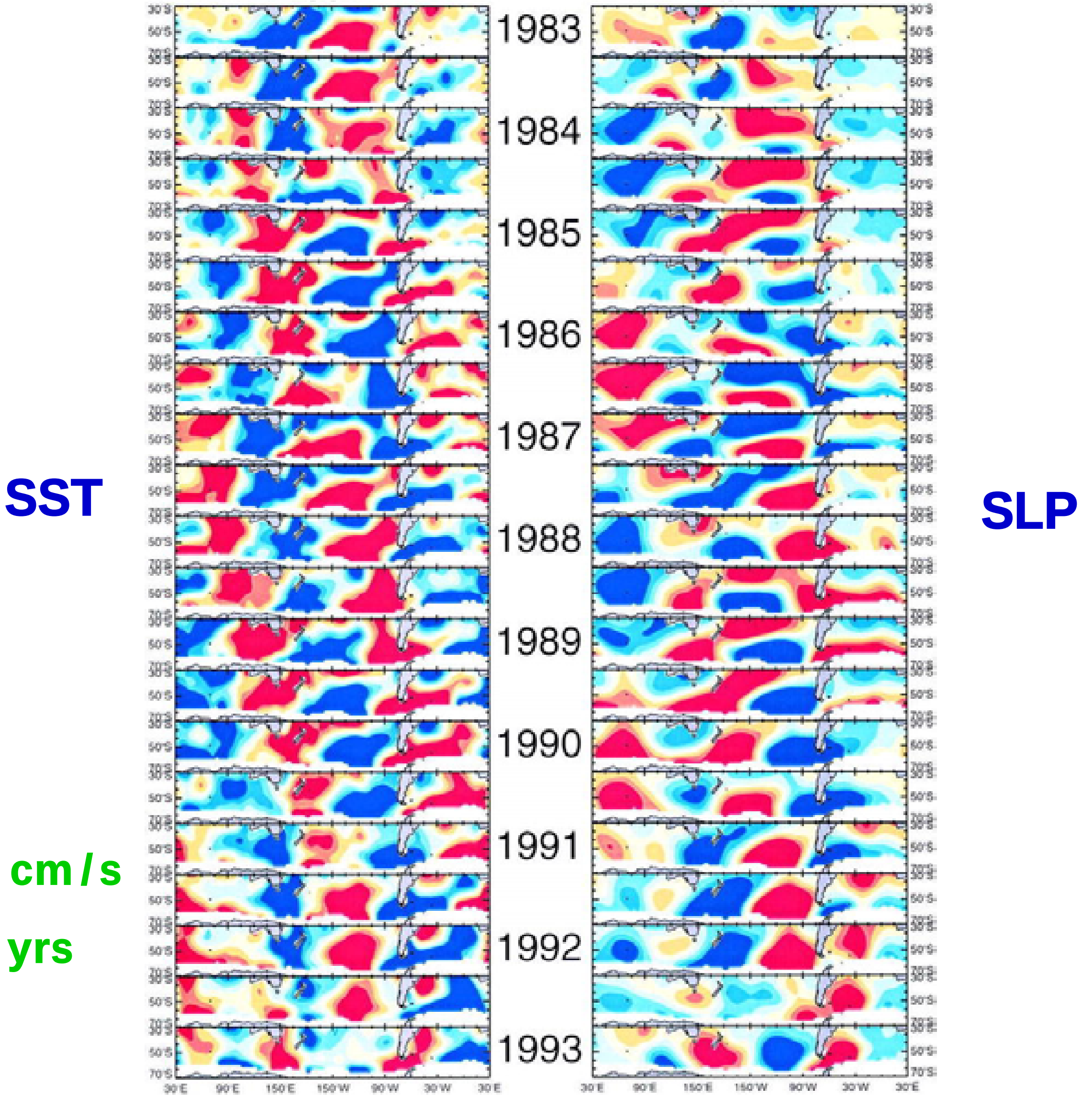

phase speed = 6~8 cm/s

wave period = 4~5 yrs

wavenumber = 2

Dynamic Models for ACWs

- White and Peterson (1996): Nature, 380, 699-702
- Jacobs and Mitchell (1996): GRL, 23, 2947-2950
- Qiu and Jin (1997): GRL, 24, 2585-2588
- Christoph et al. (1998): JClim,11, 1659-1672
- White et al. (1998): JPO, 28, 2345-2361
- Cai et al. (1999): JClim, 12, 3087-3104
- Baines and Cai (2000): JClim, 13, 1831-1844
- Carril and Navarra (2001): GRL, 28, 4623-4626
- White and Chen (2002): JClim, 16, 2577-2596
- Venegas (2003): JClim, 16, 2509-2525

Jacobs and Mitchell (1996)

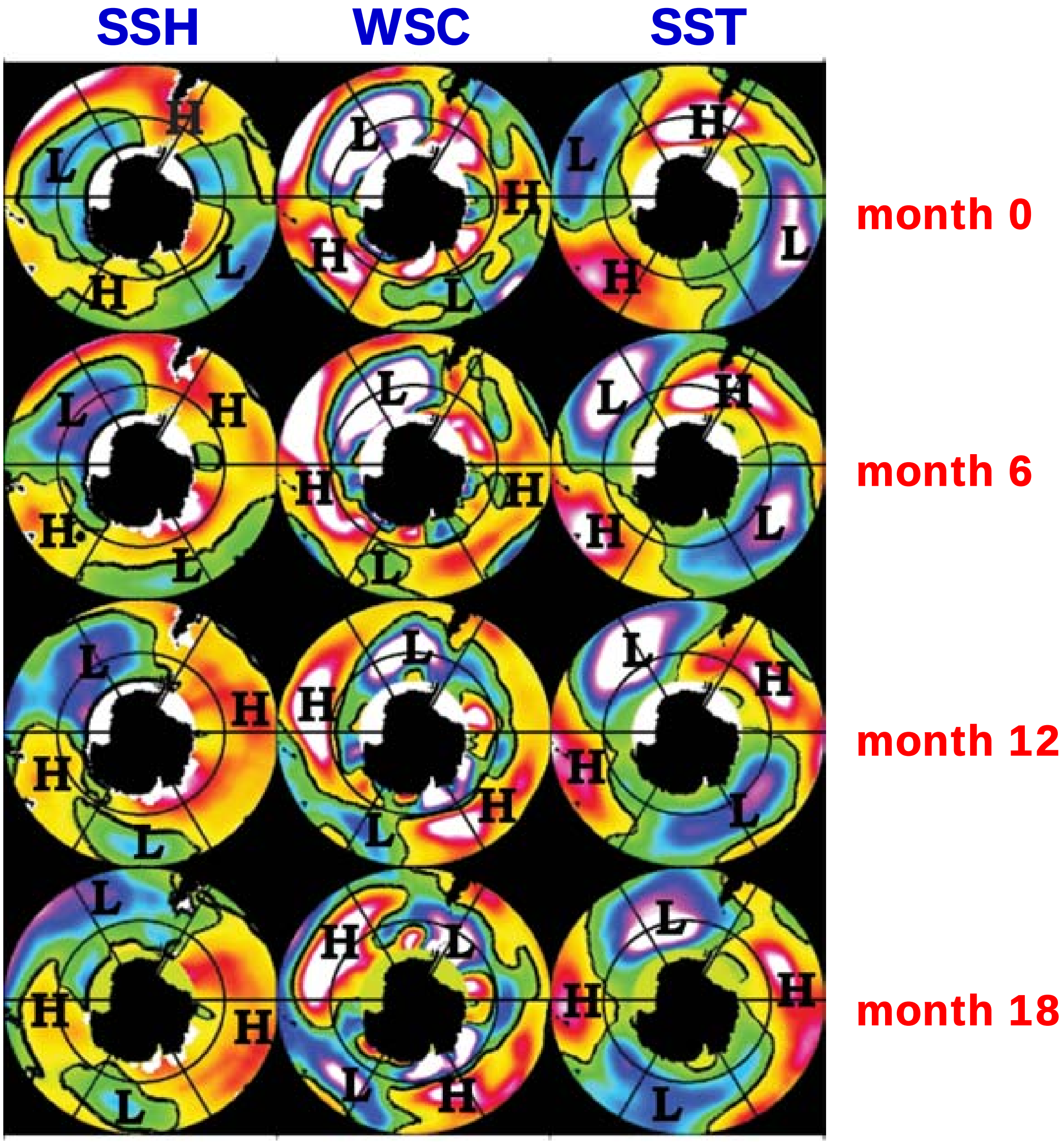

A Simple Ocean-Atmos. Model for the Southern Ocean

- **ACC: wind-driven, 2-layer QG model**

$$\boxed{\begin{aligned}\left(\frac{\partial}{\partial t}+U_1\frac{\partial}{\partial x}\right)(\phi_1-\phi_2)-(c_1+U_1-U_2)\frac{\partial\phi_1}{\partial x} &= -\frac{g'}{\rho_o f_o}\nabla\times\vec{\tau}\\ \left(\frac{\partial}{\partial t}+U_2\frac{\partial}{\partial x}\right)(\phi_1-\phi_2)+(c_2-U_1+U_2)\frac{\partial\phi_2}{\partial x} &= 0,\end{aligned}}$$

$$\begin{aligned}\text{mean zonal flows}: &\quad U_i\\ &\quad c_i=\beta g' H_i/f_o^2\\ \text{anomalous wind stress}: &\quad \vec{\tau}/\rho_o=\epsilon(\vec{k}\times\nabla p')/\rho_a f_o\end{aligned}$$

- **SST:**

$$\boxed{\left(\frac{\partial}{\partial t}+U_1\frac{\partial}{\partial x}\right)T'+\frac{1}{f_o}\frac{\partial\phi_1}{\partial x}\bar{T}_y-\frac{\tau^x}{\rho_o f_o h}\bar{T}_y = Q',}$$

$$\begin{aligned}\text{mean SST gradient across ACC}: &\quad \bar{T}_y\\ \text{anomalous heat flux}: &\quad Q'=\kappa_o(T_a'-T')\end{aligned}$$

- **Atmospheric: heat balance in lower troposphere equilibrated with the oceanic state**

$$\boxed{U_a\frac{\partial T_a'}{\partial x}+v_a'\frac{\partial\bar{T}_a}{\partial y} = -\frac{\kappa_a}{\kappa_o}Q',}$$

$$\begin{aligned} &\quad v_a'=(\partial p'/\partial x)/\rho_a f_o\\ \text{equivalent barotropic}: &\quad p'=\lambda T_a'\end{aligned}$$

A Passive Ocean Scenario:

$$\left(\frac{\partial}{\partial t}+U_1\frac{\partial}{\partial x}\right)(\phi_1-\phi_2)-(c_1+U_1-U_2)\frac{\partial\phi_1}{\partial x}=-A\nabla^2 p'$$
$$\left(\frac{\partial}{\partial t}+U_2\frac{\partial}{\partial x}\right)(\phi_1-\phi_2)+(c_2-U_1+U_2)\frac{\partial\phi_2}{\partial x}=0$$
$$\left(\frac{\partial}{\partial t}+U_1\frac{\partial}{\partial x}\right)T'-D\frac{\partial\phi_1}{\partial x}-E\frac{\partial p'}{\partial y}=\kappa_o\left(\frac{p'}{\lambda}-T'\right)$$

where

$$A = g'\epsilon/\rho_a f_o^2$$
$$D = -\bar{T}_y/f_o$$
$$E = -\epsilon\bar{T}_y/\rho_a f_o^2 h$$

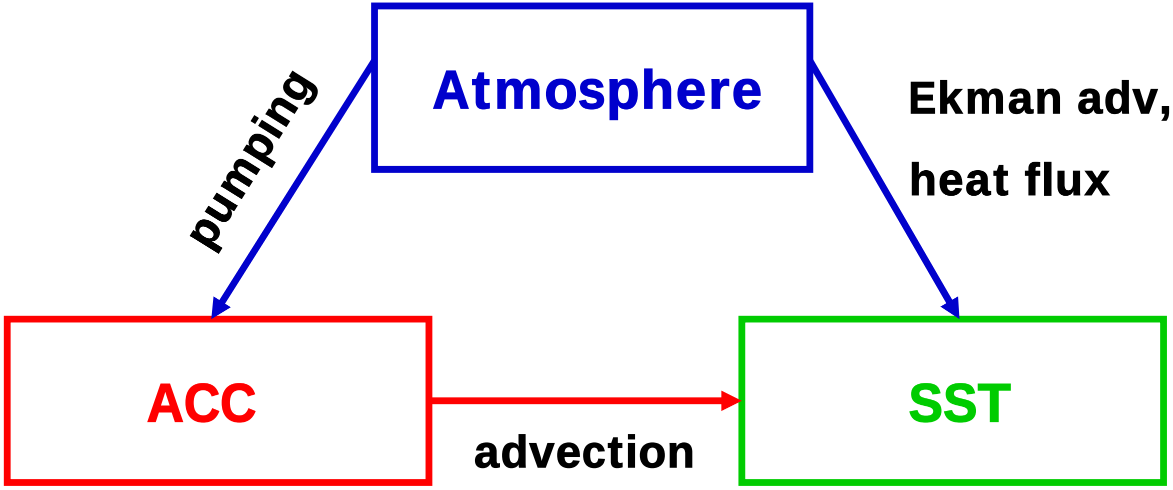

- Assume $p' \propto \exp i\,(kx + ly - \omega t)$:

$$\phi_1' = \frac{iA(k^2+l^2)(c - U_1 + c_2)}{k(c_1+c_2)(c-c_R)}\, p'$$

$$T' = \frac{1}{(\kappa_o - i\omega + ikU_1)}\left[\frac{\kappa_o}{\lambda} - ilE + \frac{DA(k^2+l^2)(c-U_1+c_2)}{(c_1+c_2)(c-c_R)}\right] p'$$

where

$$c_R = \frac{H_1U_1 + H_2U_2}{H_1 + H_2} - \frac{\beta g' H_1 H_2}{f_o^2(H_1+H_2)}$$

is the Rossby wave speed of the 2-layer ACC system.

- For parameter values appropriate for the Southern Ocean and with $k = 2$, $2\pi/\omega = 4.5$ yrs.:

Forced Mode (k=2)

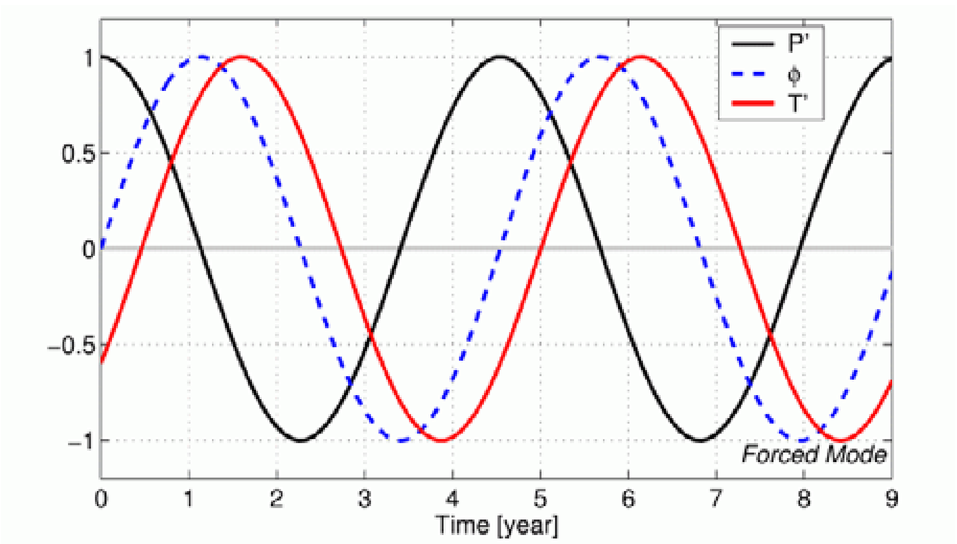

A Coupled System Scenario:

$$\left(\frac{\partial}{\partial t}+U_1\frac{\partial}{\partial x}\right)(\phi_1-\phi_2)-(c_1+U_1-U_2)\frac{\partial\phi_1}{\partial x}=-A\nabla^2 p'$$
$$\left(\frac{\partial}{\partial t}+U_2\frac{\partial}{\partial x}\right)(\phi_1-\phi_2)+(c_2-U_1+U_2)\frac{\partial\phi_2}{\partial x}=0$$
$$\left(\frac{\partial}{\partial t}+U_1\frac{\partial}{\partial x}\right)T'-D\frac{\partial\phi_1}{\partial x}-E\frac{\partial p'}{\partial y}=\kappa_o\left(\frac{p'}{\lambda}-T'\right)$$
$$U_a^*\frac{\partial p'}{\partial x}=-\frac{\kappa_a}{\kappa_o}\left(\frac{p'}{\lambda}-T'\right)$$

where $U_a^* = U_a + \lambda\bar{T}_{ay}/\rho_a f_o$

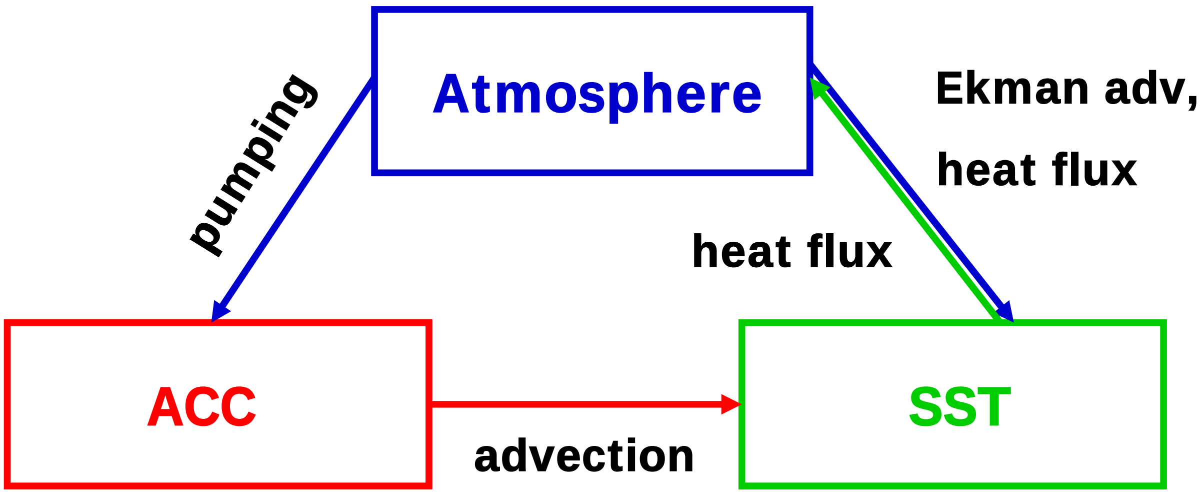

- **Assuming** $p' \propto \exp i\,(kx + ly - \omega t)$ **leads to the dispersion relation:**

$$\boxed{(\omega - \omega_R)(\omega - \omega_S) + \frac{\kappa_a AD(k^2 + l^2)(\omega + kc_2 - kU_1)}{\kappa_o(kU_a^* - i\kappa_a)(c_1 + c_2)} = 0}$$

- **If** $\kappa_a = 0$ **(uncoupled system):**

$$\omega_1 = \omega_R \equiv k\left[\frac{H_1U_1 + H_2U_2}{H_1 + H_2} - \frac{\beta g' H_1 H_2}{f_o^2(H_1 + H_2)}\right]$$

$\Rightarrow$ **neutral baroclinic Rossby mode in sheared ACC**

$$\omega_2 = \omega_S \equiv kU_1 - i\kappa_o \frac{\kappa_a(ilE + \kappa_o/\lambda)}{\kappa_o(kU_a^* - i\kappa_a)}$$

$\Rightarrow$ **decaying SST mode**

- **When** $\kappa_a \neq 0$, **the coupled Rossby mode is unstable for parameter values appropriate for the Southern Ocean and its overlying atmosphere.**

- **Parameter values appropriate for the Southern Ocean and atmosphere (based on WOA01, NCEP reanalysis data):**

$f_o = -1.19 \times 10^{-4}\mathrm{s}^{-1}$	$\pi/l = 10°\mathrm{lat.}$	$g' = 0.015\ \mathrm{m\,s^{-2}}$
$\beta = 1.32 \times 10^{-11}\mathrm{s}^{-1}\mathrm{m}^{-1}$	$H_1 = 500\ \mathrm{m}$	$H_2 = 4500\ \mathrm{m}$
$\bar{T}_y = 0.4°\mathrm{C}/°\mathrm{lat.}$	$\bar{T}_{ay} = 0.4°\mathrm{C}/°\mathrm{lat.}$	$h = 200\ \mathrm{m}$
$U_1 = 0.12\ \mathrm{m\,s^{-1}}$	$U_2 = 0.08\ \mathrm{m\,s^{-1}}$	$U_a^* = 5.0\ \mathrm{m\,s^{-1}}$
$\epsilon = 0.9 \times 10^{-5}\ \mathrm{m\,s^{-1}}$	$\kappa_o^{-1} = 2\ \mathrm{yrs.}$	$\kappa_a^{-1} = 2\ \mathrm{weeks}$
$\lambda = 400\ \mathrm{N\,m^{-1}\,°C^{-1}}$		

Coupled Mode

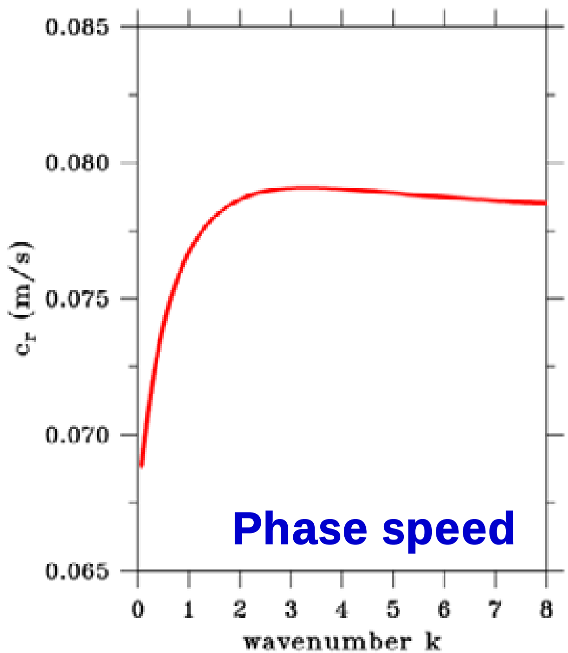

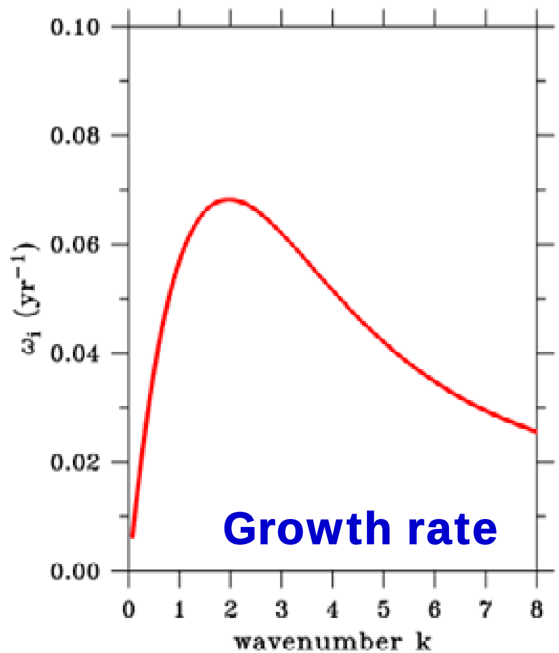

Coupled Mode (k=2)

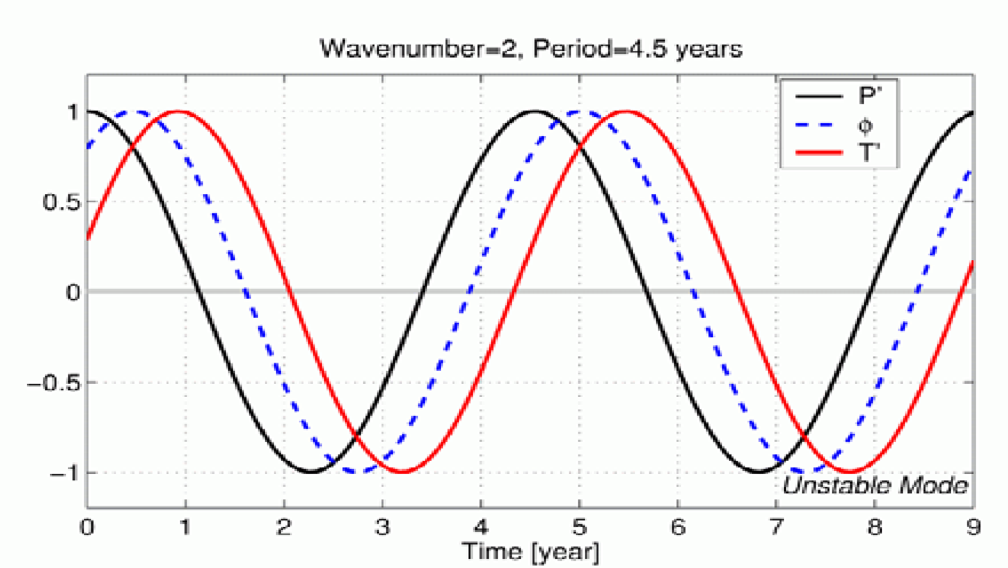

Forced Mode (k=2)

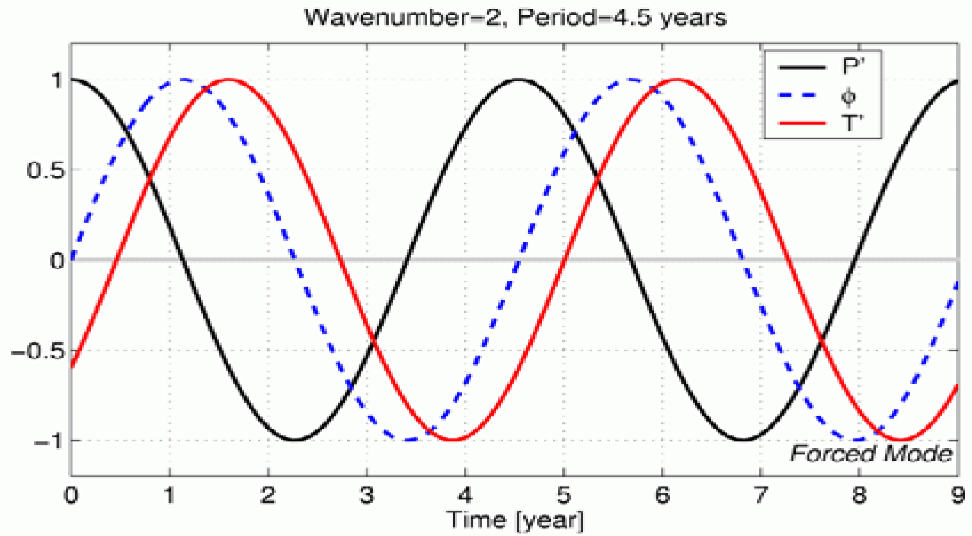

Coupled Mode (k=2)

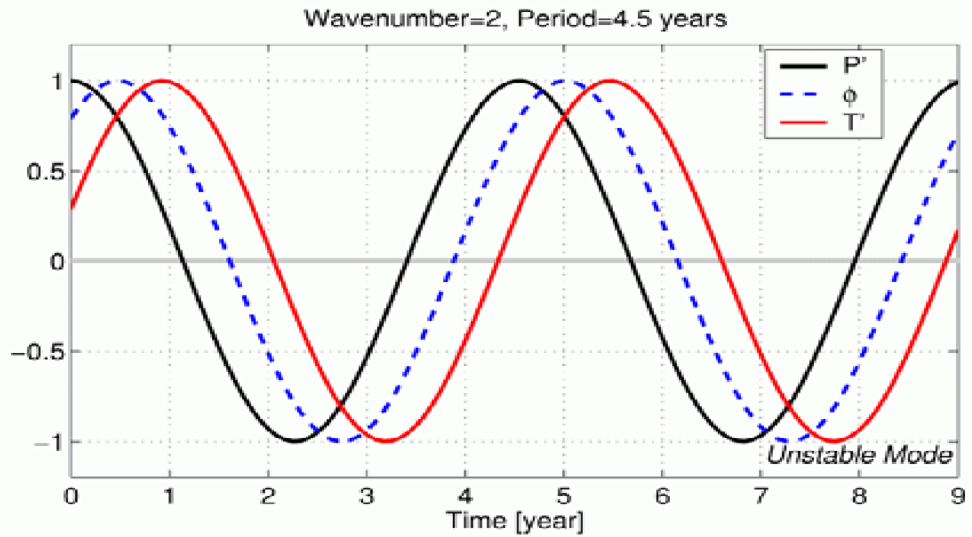

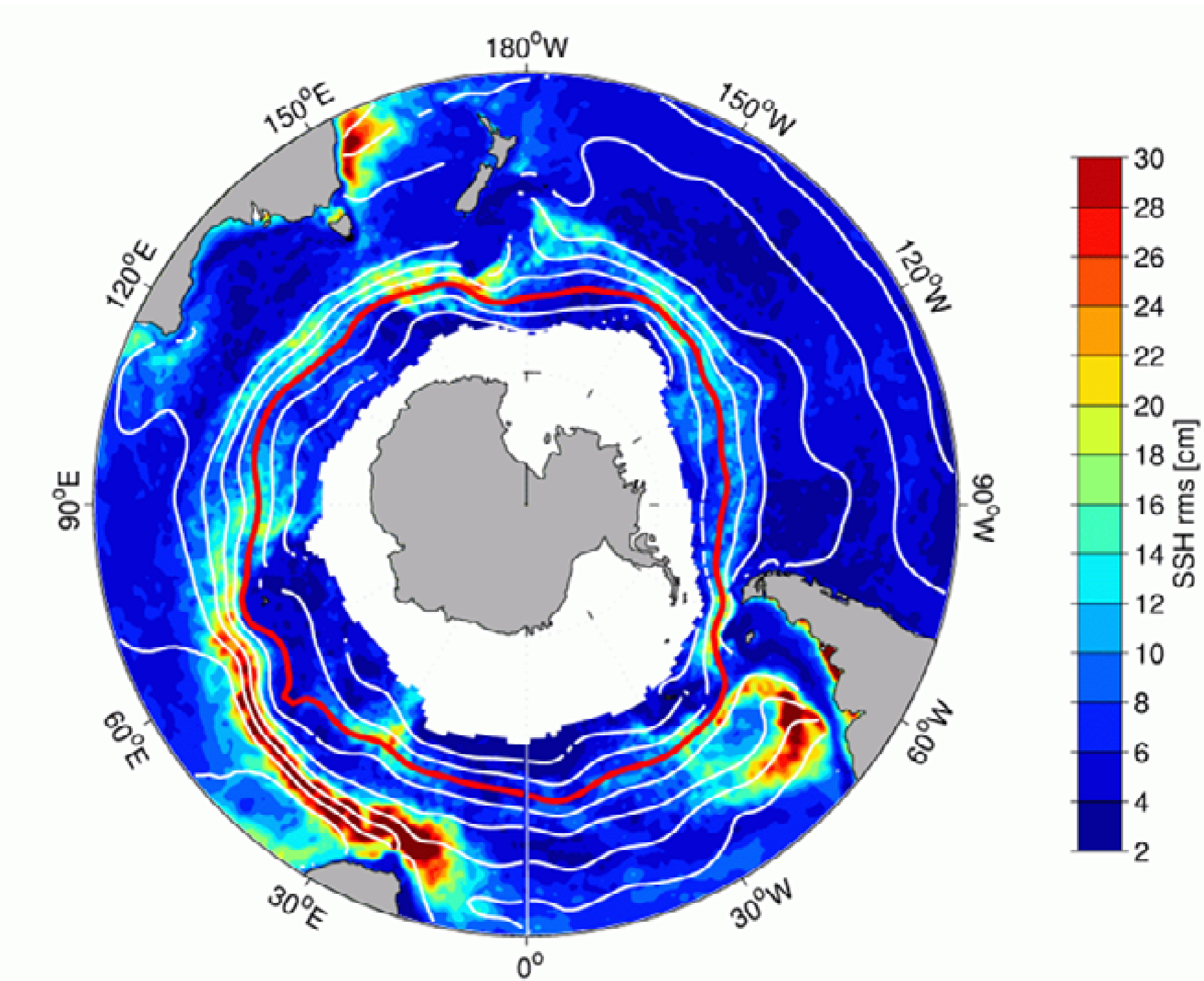

(contours: mean SSH; red: ACC path center)

SST, SSH and SLP Anomalies along the ACC Band

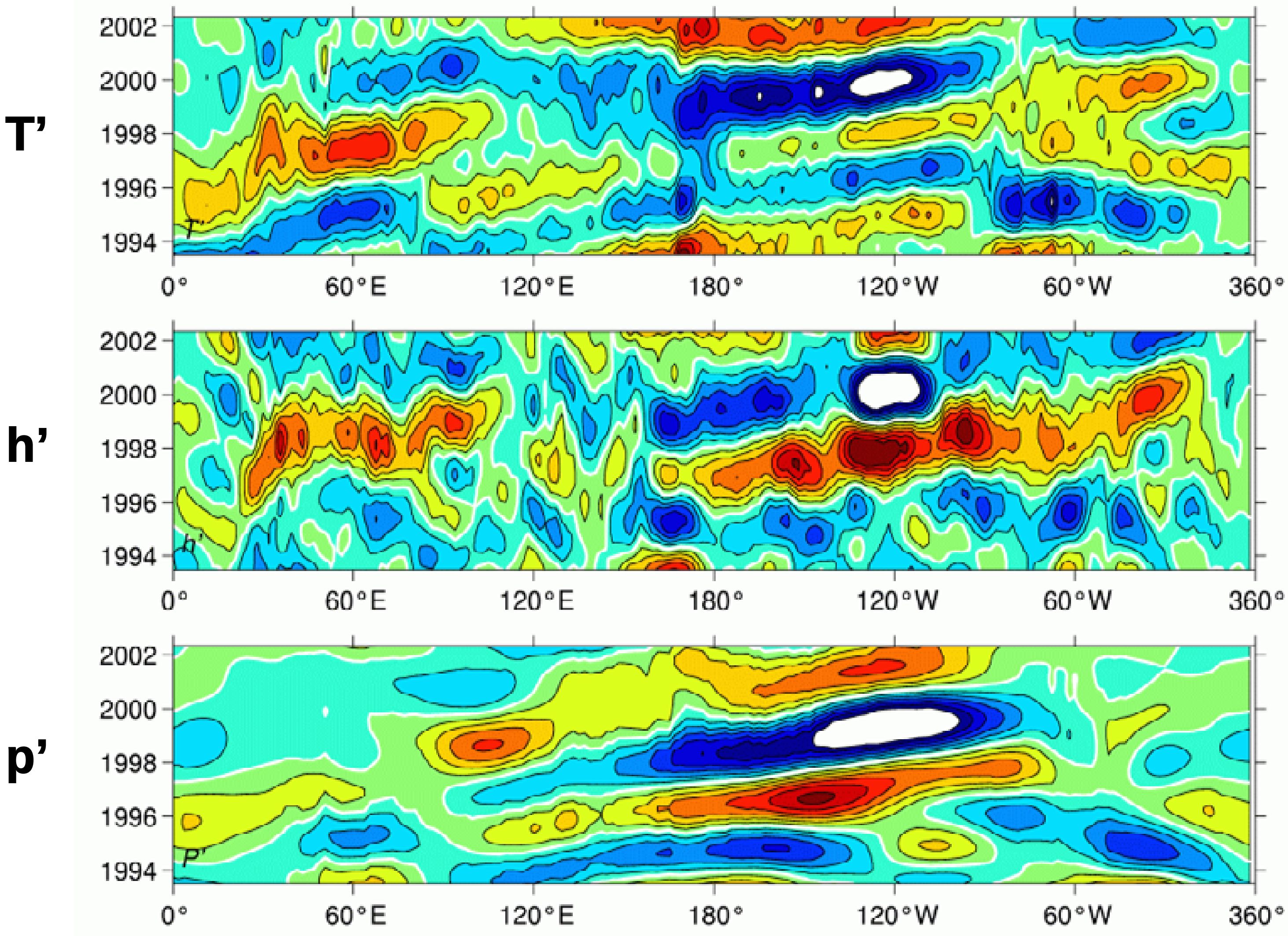

Joint CEOF Mode-1 Anomalies along the ACC Band

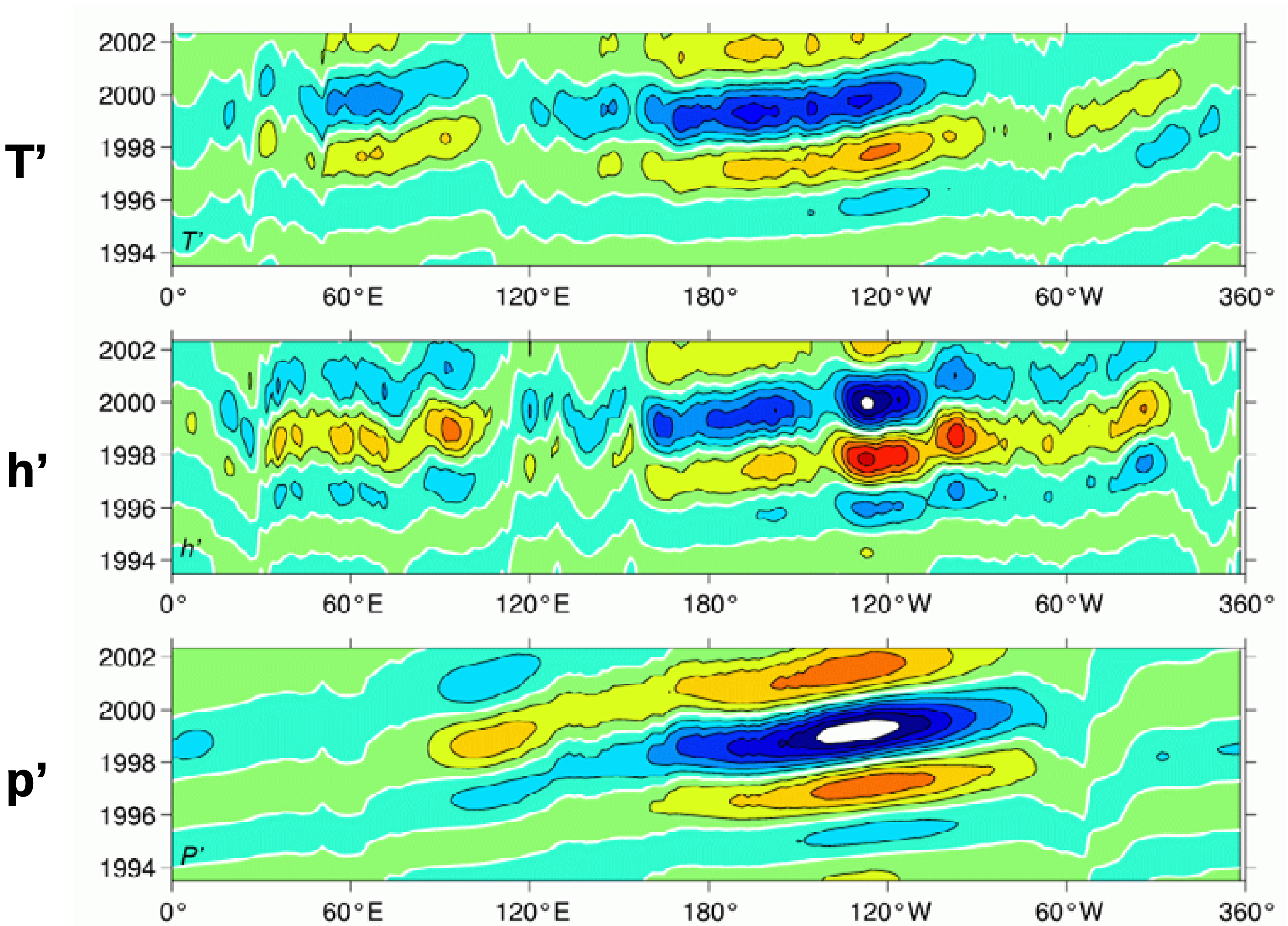

Observed Phases

Along 110W

(CEOF Mode-1)

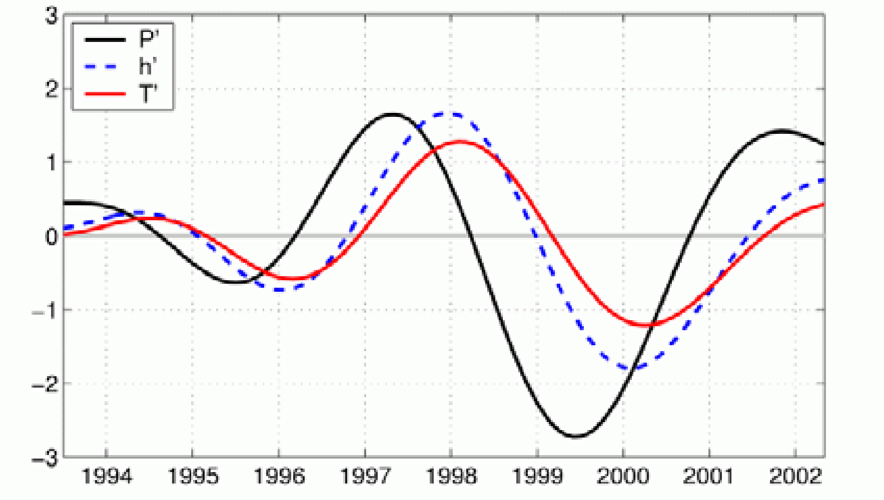

Observed Phases Along 110W (CEOF Mode-1)

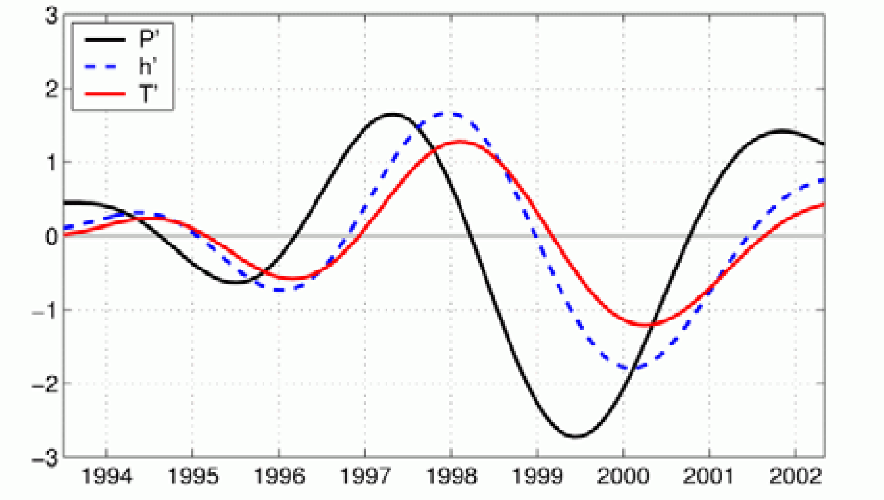

Forced Mode

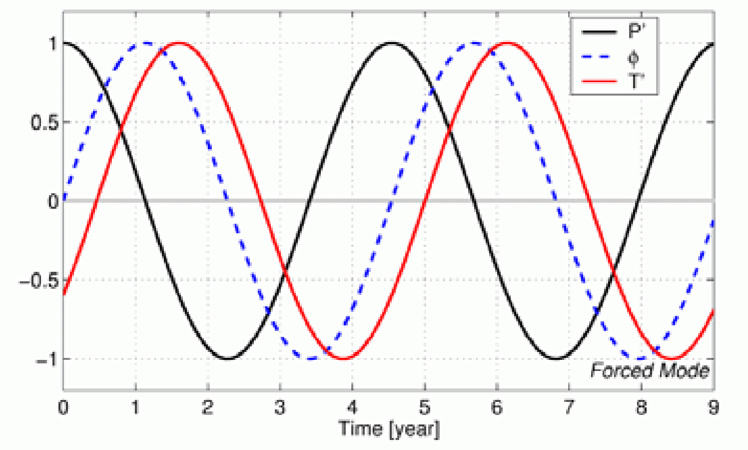

Coupled Mode

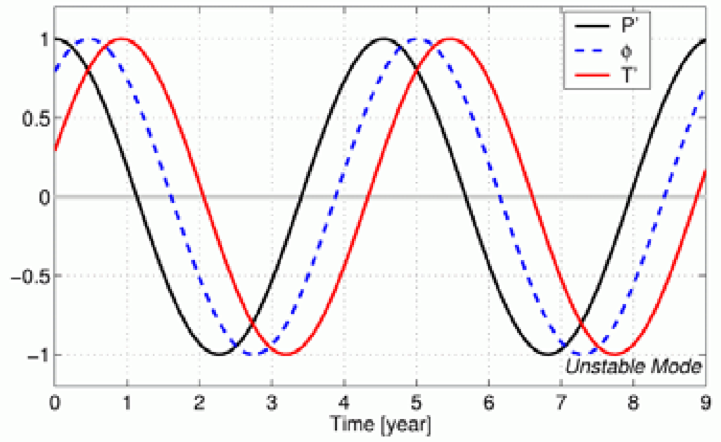

Summary of Point 2

- Altimetrically-derived SSH signals are an important dynamic variable and can be used to test physical hypotheses of an observed phenomenon.
- The decade-long SSH data indicates that the oceanic ACWs are better described as coupled signals rather than as passive signals forced by the atmosphere.
- As with other low-frequency climate signals, longer SSH measurements are desired to confirm the coupled nature of the ACWs.

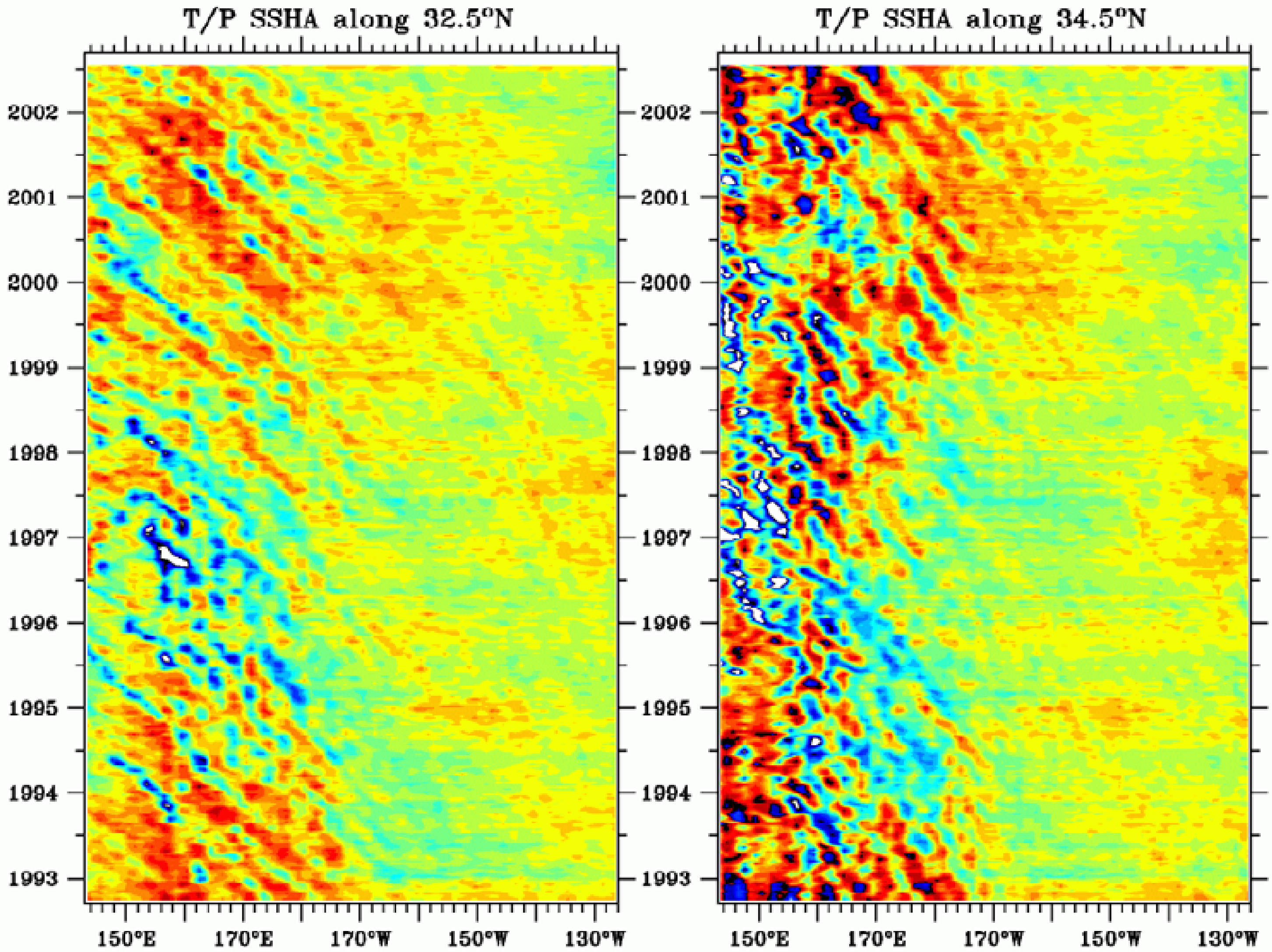
T/P SSHA along 32.5°N
T/P SSHA along 34.5°N
2002
2001
2000
1999
1998
1997
1996
1995
1994
1993
150°E
170°E
170°W
150°W
130°W

Ray paths

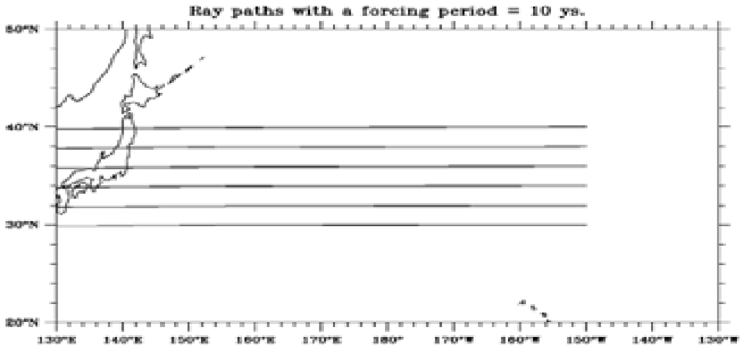

T= 10 yr.

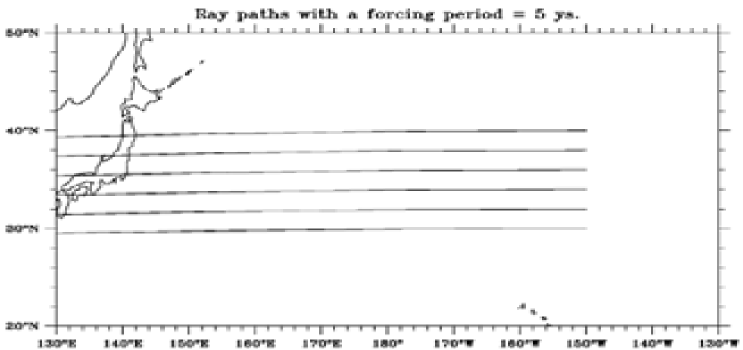

T = 5 yr.

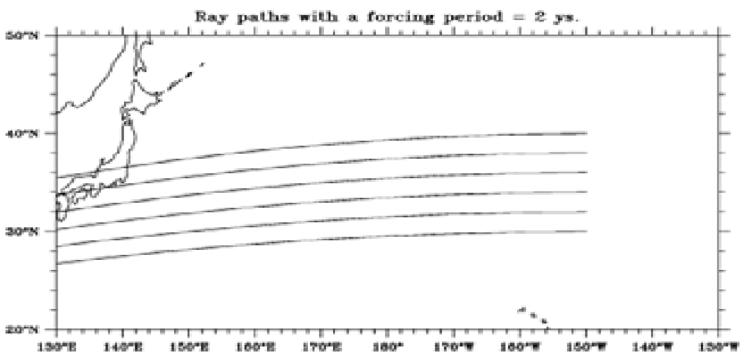

T = 2 yr.